

Article

Techno-Economic and Environmental Impact Analysis of Large-Scale Wind Farms Integration in Weak Transmission Grid from Mid-Career Repowering Perspective

Rohan Zafar Butt ¹, Syed Ali Abbas Kazmi ¹, Mohammed Alghassab ^{2,*}, Zafar A. Khan ^{3,4},
Abdullah Altamimi ⁵, Muhammad Imran ⁶ and Fahad F. Alruwaili ⁷

- ¹ US-Pakistan Center for Advanced Studies in Energy (USPCAS-E), National University of Sciences and Technology (NUST), H-12, Islamabad 44000, Pakistan; rohaanzb@gmail.com (R.Z.B.); saakazmi@uspcase.nust.edu.pk (S.A.A.K.)
 - ² Department of Electrical and Computer Engineering, Shaqra University, Riyadh 11911, Saudi Arabia
 - ³ Department of Electrical Engineering, Mirpur University of Science and Technology, Mirpur AJK 10250, Pakistan; zafarakhan@ieee.org
 - ⁴ School of Computing and Engineering, Institute for Innovation in Sustainable Engineering, University of Derby, Derby DE22 1GB, UK
 - ⁵ Department of Electrical Engineering, College of Engineering, Majmaah University, Al-Majmaah 11952, Saudi Arabia; a.altmimi@mu.edu.sa
 - ⁶ School of Engineering and Applied Science, Mechanical Engineering and Design, Aston University, Birmingham B4 7ET, UK; m.imran12@aston.ac.uk
 - ⁷ College of Computing and Information Technology, Shaqra University, Riyadh 11911, Saudi Arabia; alruwaili@su.edu.sa
- * Correspondence: malghassab@su.edu.sa



Citation: Butt, R.Z.; Kazmi, S.A.A.; Alghassab, M.; Khan, Z.A.; Altamimi, A.; Imran, M.; Alruwaili, F.F. Techno-Economic and Environmental Impact Analysis of Large-Scale Wind Farms Integration in Weak Transmission Grid from Mid-Career Repowering Perspective. *Sustainability* **2022**, *14*, 2507. <https://doi.org/10.3390/su14052507>

Academic Editor: Detlef Schulz

Received: 7 December 2021

Accepted: 7 February 2022

Published: 22 February 2022

Publisher's Note: MDPI stays neutral with regard to jurisdictional claims in published maps and institutional affiliations.



Copyright: © 2022 by the authors. Licensee MDPI, Basel, Switzerland. This article is an open access article distributed under the terms and conditions of the Creative Commons Attribution (CC BY) license (<https://creativecommons.org/licenses/by/4.0/>).

Abstract: Repowering a wind farm enhances its ability to generate electricity, allowing it to better utilize areas with high mean wind speeds. Pakistan's present energy dilemma is a serious impediment to its economic development. The usage of a diesel generator as a dependable backup power source raises the cost of energy per kWh and increases environmental emissions. To minimize environmental emissions, grid-connected wind farms enhance the percentage of wind energy in the electricity system. These wind generators' effects, on the other hand, are augmented by the absorption of greater quantities of reactive electricity from the grid. According to respective grid codes, integration of commercial onshore Large-Scale Wind Farms (LSWF) into a national grid is fraught with technical problems and inter-farm wake effects, which primarily ensure power quality while degrading overall system operation and limiting the optimal use of attainable wind resources. The goal of this study is to examine and estimate the techno-economic influence of large-scale wind farms linked to poor transmission systems in Pakistan, contemplating the inter-farm wake effect and reactive power diminution and compensating using a range of voltage-ampere reactive (VAR) devices. This study presents a partial repowering technique to address active power deficits produced by the wake effect by raising hub height by 20 m, which contributed to recovering the active power deficit to 48% and so reduced the effects of upstream wind farms. Simulations were conducted for several scenarios on an actual test system modeled in MATLAB for comparative study using capacitor banks and different flexible alternating current transmission system (FACTS) devices. Using the SAM (System Advisor Model) and RETScreen, a complete technical, economic, and environmental study was done based on energy fed into the grid, payback time, net present value (NPV), and greenhouse gases (GHG) emission reduction. The studies suggest that the unified power flow controller (UPFC) is the optimum compensating device via comparison analysis as it improved the power handling capabilities of the power system. Our best-case scenario includes UPFC with hub height augmentation, demonstrating that it is technically, fiscally, and environmentally viable. Over the course of its lifespan, the planned system has the potential to save 1,011,957 tCO₂, resulting in a greener environment. When the energy generated annually by a current wake-affected system is compared to our best-recommended scenario, a recovered shortfall of 4.851% is seen, with improved system stability. This modest investment in repowering boosts energy production due to wake effects, resulting in increased NPV, revenue, and fewer CO₂ footprints.

Keywords: renewable energy; system advisor model; transmission grid; wind generation

1. Introduction

Energy is a very important factor in ensuring economic and social growth. Resources and the environment are becoming more significant constraints on energy generation as fossil fuels deplete and the threat of climate change intensifies. The major problems that the globe faces today are environmental security, energy resource conservation, and sustainable energy production. Because of population growth and industrialization, power consumption is continually increasing [1,2]. The only solution to this catastrophe, to develop sustainable energy, is all over the world [3]. Wind energy has grown rapidly during the previous two decades, with a global total installed wind power capacity surpassing 733 GW in 2021 [4]. Because of the unpredictable and stochastic nature of wind, the vast quantity of wind power generation poses significant problems to the steady functioning of power networks. Many hurdles face the integration of LSWF into national transmission systems in many countries, including technical, economic, and environmental considerations [5,6].

In 1978, Denmark erected the first onshore multi-megawatt wind turbines [7], which were largely erected on farmland, allowing for cost-effective joint-use projects near the sea to take benefit of higher coastal wind profiles [8]. Offshore wind has the potential to be a significant technology because of its greater capacity factors [9]. Recent advancements in offshore foundations have enabled the deployment of wind turbines in deeper seas, increasing the worldwide offshore wind potential [10]. At the end of 2019, Germany had the most onshore wind capacity in Europe, with 54 GW, while the UK had the most offshore wind capacity, with 11 GW, followed by Germany (7.6 GW) at the end of 2020 [11,12]. After years of study and development, emerging nations have devised novel solutions and improved their grid codes and infrastructure to account for wind risks [13]. Developing nations, on the other hand, continue to suffer from insufficient grid infrastructure, particularly in terms of LSWF integration.

Resource integration, power quality (PQ) as per grid codes, and reactive power correction, as well as forecasting and the wake effect, have all been investigated as technical, economic, and environmental elements of wind farms (WFs) integration. Such improvements in power would not only improve the financial payback on the development of wind farms but would also improve the competitive pricing of wind power usage [14]. Repowering a wind farm entails either changing the existing turbines with brand new and more competent ones towards the end of their mean life cycle or installing new, more efficient (20 years) turbines [15] or the midlife restoration of current degraded turbines [16] to enhance their energy-generating capacity. Changing the heights of hub-impacted turbines might thus be a potential choice for improving energy production [17]. Inter-farm wake impact has been studied from a variety of angles, including the distance between WTs and the decrease in wind speed caused by upstream WTs, the proportion of generation deficiency, as well as the overall efficiency of the LSWF [18–21]. Additionally, it is confirmed that a rise in overall power production and a reduction in turbulence can be achieved with different hub heights.

To maintain voltage levels under acceptable ranges, severe wind speed changes were resolved in [22], utilizing active (P) and reactive (Q) power-coordinated controllers established on multi-scale model predictive control theory. Wake effect and wind intermittency amplify PQ concerns in LSWF, resulting in variable output power that affects voltage stability [23,24], frequency stability [24], harmonics [23], fault ride-through [25], and power factor [26]. The incorporation of the LSWF into transmission grids raises the risk of Q compensation issues, which have been studied in a variety of situations for a variety of applications, most notably in FACTS. Reactive power compensators such as capacitor banks and reactor banks are often employed to maintain voltage and PF; however, they emit high-frequency harmonics and severe switching transients [27]. SVCs provide for real-time

Q-control as well as grid voltage and PF stabilization; they lack dampening mechanisms. As a consequence, voltage overshoots may cause a cascade of WTs to trip [28]. The static synchronous compensator (STATCOM) incorporates a damping mechanism that solves the concerns of SVC, resulting in improved power quality and stability [29]. UPFC can manage both active and reactive power flows, increasing the system's stability rapidly and constantly [30]. Furthermore, in different evaluation scenarios, the static synchronous series compensator (SSSC), UPFC, and STATCOM all result in enhanced Q compensations and have a positive impact on voltage profiles and load flows [25,31].

The WTG is created on types such as the doubly-fed induction generator (DFIG), squirrel-cage induction generator (SCIG), and wound rotor synchronous generator (WRSG) [6,26,32]. Because of its low cost and high performance, the DFIG is frequently employed in wind farms [33,34]. Wind-based renewable energy sources (RESs) have been increasingly integrated into the national grid and used in the energy market in recent decades [35]. However, their naturally intermittent nature can pose problems for grid operators in terms of forecasting and meeting load [36,37]. Energy storage devices established on hydrogen for WF are one of the alternatives proposed throughout the years to alleviate such issues (ESSs) [38–40].

Wind turbines are typically intended to have a 20–25-year service life; several studies have looked at the techno-economic viability of WF, but only a few have gone into the end of their mean life scenarios in-depth [41–43]. During the lifespan of the system, the NPV idea is used to correspond to the total present value of cash flow, which includes the initial expense of all components, replacement costs, maintenance expenses, investment costs, and discount costs [44]. The LCOE is a widely used economic measure for comparing various energy technologies [45]. The LCOE displays the price of generated energy rather than estimating the prospective profit of an investment, which may be evaluated using other economic measures such as return on investment and internal rate of return (IRR) [46].

Global warming and climate change have been driven by a rise in the concentration of CO₂ during the previous few years, posing a danger to environmental sustainability [47]. According to research from the European Commission's Joint Research Centre (JRC), the burning of fossil fuels accounts for around 90% of total world CO₂ emissions [48]. Following these matters, governments adopted the Kyoto and Paris climate contracts to limit greenhouse gas production. Pakistan ratified the Paris Agreement on 11 November 2016, nearly precisely one year after submitting its climate pledge, or "nationally determined contribution" (NDC), to the Paris climate summit. Pakistan's 2025 vision climate and energy framework established objectives for improving at least 32% of renewable energy proportion and improving at least 32.5% of energy efficiency [49]. Technological innovation helps stabilize the economy and pushes countries to embrace contemporary development plans that reduce CO₂ emissions [50,51]. Researchers have assessed the greenhouse gas emissions of wind-generating plants in the United States [52], Mexico [53], Jordan [54], Brazil [55], Turkey [56], Japan [57], and Libya [58].

By 2020, each member state of the European Union (EU) is expected to have a required 20% renewable energy contribution in their overall energy consumption [59]. The study in [24] explored increasing wind penetration in the power pool grid of the southwestern United States to address stability concerns such as constant voltage profiles, under-voltage ride-through capabilities with capacitors banks, and SVC as Q compensators [60]. According to estimates of industry, about 8 GW of capacity will be built by 2016 and over 18 GW by 2020, supplying around 20% of the UK's annual power consumption [61].

There is a significant study vacuum in the examined literature on the effects of growing wind penetration into Pakistan's wind corridor's transmission network as well as the related technological, economic, and environmental impact. Pakistan is an interesting case study since it is one of the few countries that has been battling a serious energy problem while only producing modest amounts of electricity. In the next five years, this deficit is expected to worsen, with a 7.5% annual growth rate. Only 34% of the rural residents and the country's overall residents (63%) have access to electricity [62,63]. The energy shortfall

caused a 2% drop in GDP. The country's power consumption is 18,000 MW, whereas the supply is 11,500 MW. The demand and supply disparity is estimated to be approximately 6500 MW [64]. The purpose of this article is to assess the efficacy of these approaches for suggested WFs in Pakistan in meeting the Grid Codes standards specified by NEPRA. This paper involves creating test systems in MATLAB/Simulink for a 155.4 MW wind farm. The actual characteristics given by the local electric company, Hyderabad Electric Supply Company (HESCO), are used to construct a genuine Pakistani power system. The primary objective of this study is to analyze the technological, economic, and environmental implications of a projected 50 MW WFs on the external grid of Pakistan. The study includes the midlife refurbishment of existing degraded turbines. Furthermore, the comparative research in [21] was restricted to power quality and compensation concerns using FACTS devices (i.e., capacitor bank, STATCOM, SVC, SSSC, and UPFC). These FACTS devices will need to be evaluated further in terms of their technological, economic, and environmental applications in LSWF in various circumstances.

Due to an uncoordinated design, previous onshore LSWF grid integration studies failed to account for the collective implications of inter-and intra-farm wake effects. Wake effects, wind intermittency, PQ, and Q compensation are all addressed in this study, which gives a technical and cost-effective guideline for FACTS devices. Capacitor banks and FACTS devices such as SVC, STATCOM, SSSC, and UPFC were used with and without renovating HUB height in the second part of their service life to increase power system stability and PQ through improved reactive power regulation with a relative efficiency evaluation. This study considers the wake effect, which occurs when wind speeds drop as it passes from one wind farm to another owing to the energy extracted from the wind. As a result of this occurrence, the energy production of subsequent wind farms drops, simulating a real-time scenario. This study looks at the reduction in carbon footprints after wind turbines have been refurbished and reach the second half of their operational life. The core contributions of the proposed paper are as follows:

1. LSWF integration in a deficient transmission grid, using Pakistan as a case study.
2. Performance and cost-benefit analysis of various FACTS devices as a problem-solving solution.
3. Scenario-based approach for dealing with PQ and Q compensation by appropriate and cost-effective FACTS devices as well as recovering power shortfalls by raising hub height with and without FACTS devices.
4. A complete techno-economic impact evaluation of LSWF integration in terms of the environment.

2. Energy Analysis

To assess the available wind sources on the location, examining the density of wind energy helps determine how much energy is accessible in the area to transform wind energy into electricity. The formula may be used to calculate the wind energy per unit area (A) in W/m^2 .

$$P = \frac{1}{2} \rho v^3 \quad (1)$$

The wind power can be computed using the Weibull probability density function [65].

$$\frac{P}{A} = \frac{1}{2} \rho \int_0^{\infty} v^3 f(v) dv = \frac{1}{2} \rho C^3 \Gamma \left(1 + \frac{3}{k} \right) \quad (2)$$

where ρ is the air density at sea level at 15 °C and 1.225 kg/m^3 atmospheric pressure, $f(v)$ is the probability of wind speed, v is the wind velocity, and k is the shape and scale parameters. Γ is the gamma function.

The following formula is used to get the adjusted monthly air density (kg/m^3):

$$\rho = \frac{\bar{P}}{\bar{T}R_d} \quad (3)$$

where \bar{T} is the monthly average temperature of air in (K°), \bar{P} is the monthly average pressure in Pascals, and R_d represents dry air gas constant. The density of the air will decrease as height and temperature increase [66].

By using (2) and (3) the wind energy density E for a given time T may be computed using (4).

$$E = P \times T \quad (4)$$

The following formula may be used to assess the annual generation of a wind power system:

$$E_u = \sum_{u=0}^{20} P \times P_{(x)} \times 8760 \quad (5)$$

$P_{(x)}$ is the probability of a wind speed of (m/s) occurring each year, as defined by

$$P_{(z)} = \left(\frac{k}{c}\right) \times \left(\frac{z}{c}\right)^{k-1} \times e^{-(\frac{z}{c})^k} \quad (6)$$

where k denotes the form factor defined by local meteorological circumstances, and c denotes the scale factor defined by wind speed.

Temperature, pressure, and other losses are considered when calculating the restructured yearly generation E_s (kWh).

$$E_s = E_U \times \frac{P_1 \times T_0}{P_0 \times T} \times (1 - \lambda_c) \times (1 - \lambda_s) \times (1 - \lambda_m) \times (1 - \lambda_d) \quad (7)$$

where P_1 is the air pressure (kPa) of the wind turbine at the location, P_0 is the standard atmospheric pressure (101.3 kPa), T is the temperature (K) of the wind turbine at the location, and T_0 is the standard absolute temperature (288.1 K), λ_c represents the array loss factor (valued at 3%), λ_s represents the airfoil loss factor (valued at 2%), λ_m represents the miscellaneous loss factor (valued at 2%), and λ_d represents the downtime loss factor (valued at 2%).

3. Economic Analysis

The financial analysis presented in this article is concerned with the evaluation of a renewable energy installation project regarding budgeting and financial factors that are used to establish the project's investment suitability as shown in Figure 1. Financial analysis is performed using SAM software in this study. The SAM is a techno-economic software model that helps people in the renewable energy industry make better decisions. C_n represents the cash flow for year n , the difference between the cash intake in year n ($C_{in,n}$) and the cash outflow in year n . ($C_{out,n}$) is used to calculate C_n , according to (8), (9), and (10), and can be used to determine these cash flows.

$$C_n = C_{in,n} - C_{out,n} \quad (8)$$

$$C_{out,n} = (C_{O\&M} + C_{per}) \times (1 + r_i)^n + C \times f_d \times \left(\frac{i_d}{1 - \frac{1}{(1+i_d)^N}} \right) \quad (9)$$

$$C_{in,n} = C_{ener} \quad (10)$$

where n is the debt term in years and r_i represents inflation rate. $C_{O\&M}$ also indicates the annual cost of operation and maintenance. The monthly expenses, or system credits, are denoted by C_{per} , whereas the entire starting cost is denoted by C . f_d is the debt ratio, while i_d is the annual debt interest rate. C_{ener} is the annual income from energy savings.

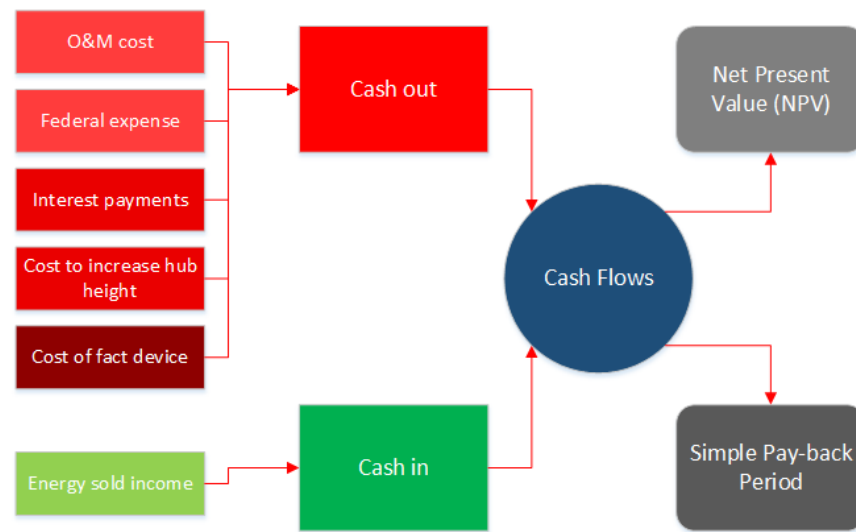


Figure 1. Block diagram of data analysis.

3.1. Simple Payback Period—SPP

The SPP is the amount of time required for the cash flow to equal the entire venture capital:

$$SPP = \frac{C}{C_{income} - C_{cost}} = \frac{C}{(C_{ener}) - (C_{O\&M})} \quad (11)$$

where C is the capital cost of the project C_{income} and (C_{ener}) is the income cost and $(C_{O\&M})$ is the operational and maintenance cost.

3.2. Net Present Value—NPV

The NPV of a project is the difference between the sum of discounted cash inflows and outflows. It is calculated by discounting all cash flows, as shown in the equation below.

$$NPV = \sum_{n=0}^N \frac{\hat{C}_n}{(1+r)^n} \quad (12)$$

where r is the discount rate of the project, and \hat{C}_n is the after-tax cash flow in n number of years.

3.3. Internal Rate of Return—IRR

The IRR is the discount rate that causes the project's NPV to be zero and is calculated by

$$\sum_{n=0}^N \frac{C_n}{(1+IRR)^n} = 0 \quad (13)$$

where C_n are the cashflows. The IRR, also known as the economic rate of return, is a rate of return that is used in capital planning to assess and analyze the profitability of investments. It is also called the "discounted cash flow rate of return" or the rate of return. The IRR is also known as the "effective interest rate" in the context of savings and loans. IRR estimates are often used to assess the viability of investments and projects. The higher the IRR of a project, the more appropriate it is to carry it through [67].

3.4. Capacitor Bank and FACTS Devices Cost Functions

The cost of installing FACTS devices has been calculated mathematically and is provided by

$$\text{Minimize IC} = C \times S \times 1000 \quad (14)$$

where IC is the ideal FACTS device installation cost in USD, and C is the cost of FACTS device installation in USD/KVAR.

Installation costs for SVC, capacitor bank, STATCOM, SSSC, and UPFC are derived from Siemens' database and provided in [68–70]. The installation costs of various FACTS devices are given by

$$C_{SVC} = 553 \times (0.0003S^2 + 0.3051S + 127.38) \quad (15)$$

$$C_{Capacitor\ bank} = 0.0004S^2 + 11S + 194.69 \quad (16)$$

$$C_{STATCOM} = 553 \times (0.0008S^2 + 0.155S + 120) \quad (17)$$

$$C_{SSSC} = -0.0001S^2 + 0.0534S + 60.86 \quad (18)$$

$$C_{UPFC} = 0.0003S^2 + 0.2691S + 188.22 \quad (19)$$

where S is the operating range of the FACTS devices in MVAR.

$$S = |Q_1| - |Q_2| \quad (20)$$

where Q_2 denotes the reactive power flow in the line after the FACTS device is installed in MVAR, and Q_1 denotes the reactive power flow in the line before the FACTS device is installed in MVAR

3.5. HUB Height Cost Function

As mentioned in [71], the cost of wind turbines accounts for around 75% of the initial capital cost (ICC) of wind farms. Towers and foundations account for around a fourth of this total. As a result, the tower and its associated foundation construction account for around 19% of the total ICC. To adapt the ICC for various tower heights, h , a base-case tower height of 80 m, is considered; a 2% increase in tower height is expected to result in a 1% rise in tower and foundation costs, owing to the increased demand for materials. As a result, wind turbine ICC may be represented as follows:

$$C_{height\ difference} = C_{100} - C_{80} \quad (21)$$

$$ICC_{(h)} = ICC_{80m} \left(1 + \frac{0.19}{2} \left(\frac{h - 80}{80} \right) \right) \quad (22)$$

where ICC_{80m} is the initial capital cost of an 80 m height wind farm. h is the height to which it is heightened.

4. Environmental Analysis

For environmental analysis in this research, RETScreen software is used. RETScreen is a decision-making tool that assists with a variety of analyses and evaluations of electricity generation and environmental effects. The model computes the net annual average decrease in GHG emissions in tons of CO₂ per year (tCO₂/year). RETScreen generates a GHG emission profile for a Base Case System (Baseline) and a Proposed Case System. The GHG emission reduction is calculated by combining the difference in the GHG emission factors with additional data generated by RETScreen. The reduction ΔGHG is calculated as follows:

$$\Delta GHG = (e_{base} - e_{prop}) E_{prop} (1 - \lambda_{prop}) \quad (23)$$

e_{base} is the base case GHG emission factor, while e_{prop} is the proposed case GHG emission factor. E_{prop} is the yearly electricity produced in the suggested scenario, and λ_{prop} is the proportion of power wasted in transmission and distribution (T&D) in the proposed case [72].

5. LSWF Test Setup and Background Information

5.1. LSWF Test Setup

Jhimpir wind energy park, located in Sindh province, is Pakistan's largest wind power producing location, with more than 18 wind turbine farms constructed and a capacity of more than 1 GW. The purpose of this study is to integrate three wind power plants into the Nooriabad grid and examine the effects of LSWF integration on transmission networks. As illustrated in Figure 2a, an actual Nooriabad grid running at 132 kV was created in SIMULINK/MATLAB (Figure 3) with three wind power plants (WPP) integrated into it, including the Fauji Fertilizer Company Energy Limited wind power plant (FFCEL), the Zorlu Enerji (ZE) Pakistan WPP, and the Three Gorges First (TGF) WPP. The FFCEL is a test case and is located downstream, whereas ZE and TGF are located upstream as shown in Figure 4. The LSWF with its respective technical specifications is shown in Table 1. The purpose of this study is to evaluate the effects of the inter-farm wake effect, which was causing active power production to deteriorate. The active power shortfall was caused by the wind slowing down as it traveled through upstream and downstream wind farms. Figure 2b depicts the FFCEL wind turbines, which are numbered according to their operating configuration. The farm's turbines 16 to 31 have a power deficiency, as detailed in [73].

FFCEL began power production in 2013, having a total capacity of 49.5 MW. The project cost was estimated by FFCEL to be USD 133.557 million. The annual O&M expenditure is USD 3 million. FFC's debt–equity ratio is 80:20 (USD 106 million and USD 28 million, respectively). The debt has a ten-year duration, while the equity has a six-year repayment period. According to FFC, at an annual net plant capacity factor of 33.11%, the total monthly benchmark energy is 143.559 GWh [74]. The project has a 20-year lifespan. For Q compensation, SVC devices were fitted. NEPRA has approved a levelized tariff of 16 US cents/kWh.

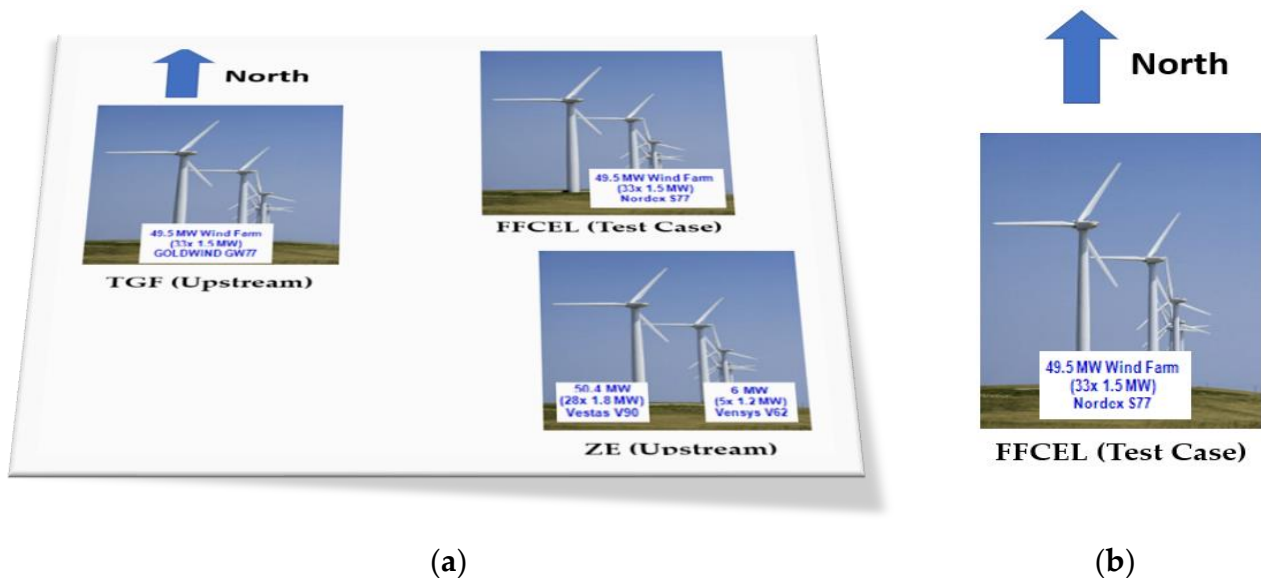


Figure 2. (a) Model of the three wind farms under consideration and (b) the FFCEL wind farm plan with operating wind turbines numbered.

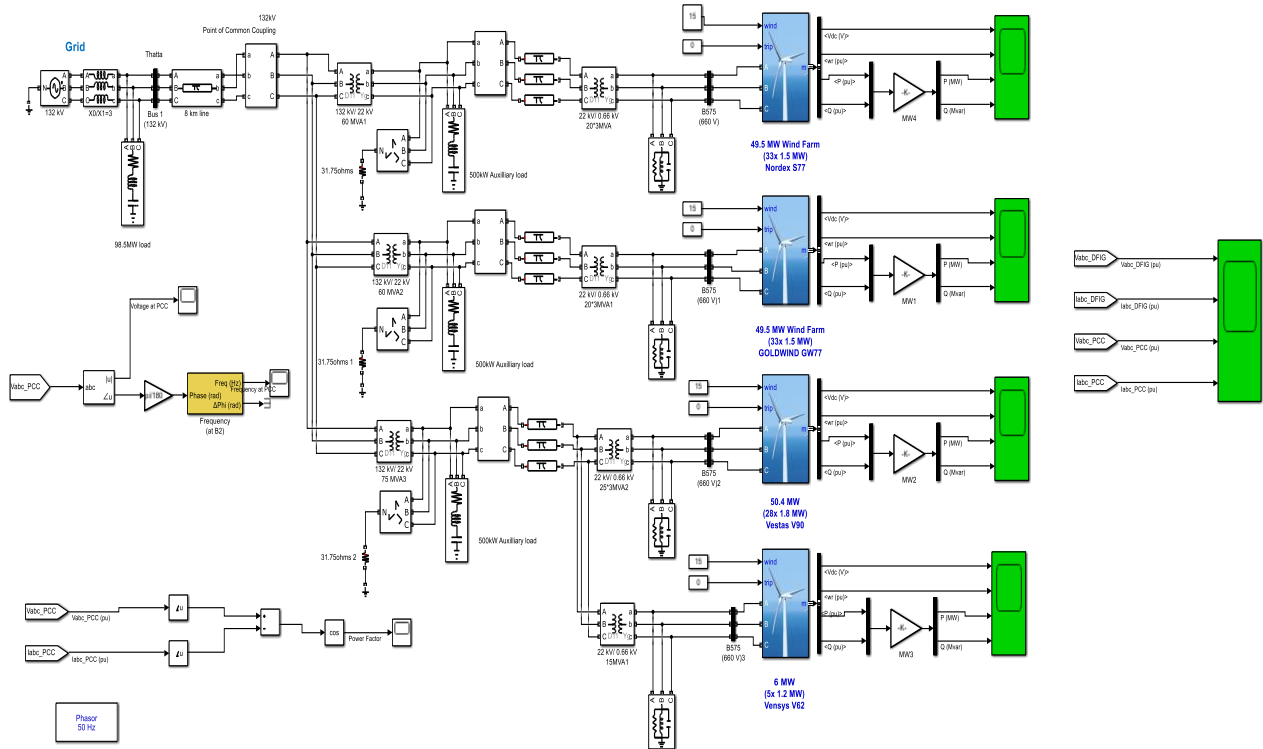


Figure 3. Base case test setup for MATLAB/SIMULINK with three interconnected wind farms [21].

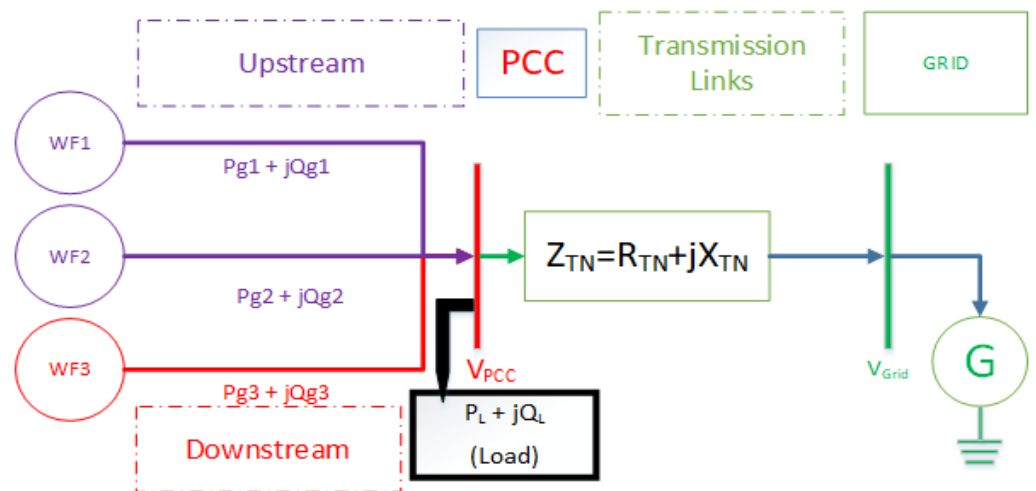


Figure 4. Equivalent of an LSWF-based model with grid integration issues.

Table 1. Technical details about test system under consideration (consisting of three WFs) [73,74].

Data	TGF (Upstream)	ZE (Upstream)	FFCEL (Test Case)
Date of Operation	November 2014	July 2013	May 2013
Turbines model	Goldwind GW771500	Vestas and Vensys-62	Nordex-S77
Turbine capacity (MW)	1.5	Vestas = 1.8; Vensys-62 = 1.2	1.5
Total number of wind turbines	33	28 × Vestas; 5 × Vensys-62	33
WF capacity (MW)	49.5	56.4	49.5
Type of Generator	DFIG	DFIG	DFIG
Generators output voltage (V)	660	660	660

The inflation rate is the percentage rise or reduction in prices over a certain time. The rate of inflation can influence project feasibility since it directly affects the payback period, the cost of energy generation, and the net present value of the system. Pakistan now has an inflation rate of approximately 12% [75], which may rise or fall in the future. The interest rate in Pakistan for renewable energy projects is fixed at 6% [76]. Inflation and interest rate are assumed at 12% and 6%, respectively, for this study. The average yearly depreciation of the Pakistani rupee versus the US dollar during the last two decades has been around 5%. Assuming the current trend continues, this aspect is also considered in this analysis as it is anticipated.

The LSWF linked with the transmission network (TN) is vulnerable to a variety of difficulties, including wind's intermittent nature, asynchronous generators (i.e., DFIG), and various stability (i.e., mostly voltage) and PQ concerns. Furthermore, Q compensation difficulties are evident in LSWF and have a direct influence on the entire system's PQ. Without any compensation, the total Q absorption of FFCEL from PS is 2.574 MVAR [21].

5.2. Grid Codes for Power Quality

The NEPRA was established to bring transparent and sensible economic control to Pakistan's electric power industry, based on solid commercial principles. The NEPRA regulates connections to Pakistan's national power system through its comprehensive Grid Codes. Non-compliance with any provisions of this grid code by any code participant is considered a breach of the grid code and shall be subject to penalties by NEPRA fees and fines regulations [77–79]. The grid codes of Pakistan's NEPRA are [80] summarized in Table 2.

Table 2. Technical details about test system under consideration (consisting of three WFs) [73,74].

Parameters	Grid Codes
Reactive Power Control	At PCC, the wind farm should manage reactive power to keep the power factor within the required range (0.95 lagging to 0.95 leading over the whole range of plant operation).
Harmonics	Wind turbines with power converters produce harmonics. Voltage and current harmonics up to 50 times the essential power frequency may be defined according to IEC61400-21. According to widely accepted standards, the PCC's total harmonic distortion (THD) from these harmonics must be less than 5%, and there ought to be no resonance at odd-frequency harmonics.
Frequency	For the provided system frequency range, the wind farm must be able to operate constantly within 49.5 to 50.5 Hz
Resonance	Odd harmonics are harmful to the power system; hence, there should be no odd harmonics.
Voltage Control	The WF should be able to produce available power while maintaining a tolerable voltage at the grid-connection point (PCC) (75% of nominal voltage).

6. Methodology

The proposed methodology seeks to fill in the gaps in prior research on onshore LSWF grid integration studies. In recent research [21], a noteworthy attempt was made to handle PQ and Q compensation difficulties with capacitor banks and different (FACTS) devices for a specific WF. However, the research did not consider the LSWF's techno-economic analysis or environmental effect. The objective of the comparative performance evaluation is to address LSWF repowering owing to wake effects as well as a cost–benefit analysis of PQ improving system stability using capacitor banks and FACTS devices such as SVC, STATCOM, SSSC, and UPFC. On a technological level, the approach is expected to give a beneficial midterm solution for expensive long-term TN reinforcements. The

suggested technique is depicted in Figure 5 is a flow chart with three cases and with respective scenarios.

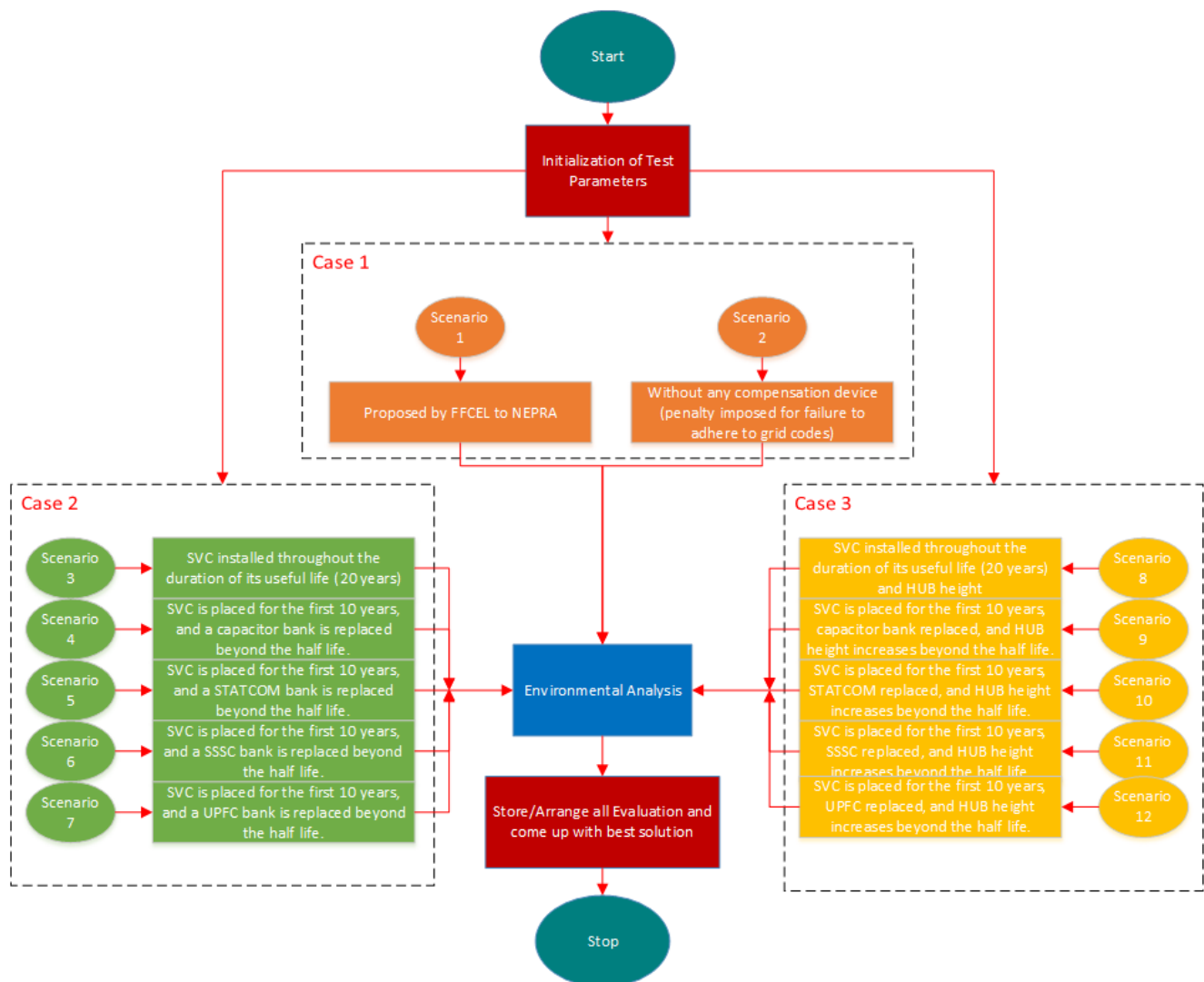


Figure 5. The suggested methodology's flow chart.

The test case (FFCEL) in this study was initiated in 2013 and has a project life of 20 years. A project's first half-life is likely to finish in 2023. In this work, a detailed techno-economic analysis of the first half-life is performed to evaluate the economic losses caused by a deficiency in PQ due to the wake effect. After the refurbishment due to wake, a techno-economic study of the second half-life is performed for a more comprehensive evaluation designed to improve power quality and reactive power compensation difficulties related to LSWF integration in poor transmission networks. The capacity of the compensating device is set to 30 MVAR for the MATLAB simulation and cost assessment, as stated in [80]. The SAM is utilized in this research to examine the economic aspects. The SAM needed data on wind speed, temperature, and the atmospheric pressure of the precise site where the WF is placed for a complete analysis. These data were gathered from a meteorological station in Jhampir City.

6.1. Case-1: Base Case Scenarios Assessment

Case-1 comprised scenarios with and without wake effects. The created base scenario (Case-1) was simulated to examine the impact of LSWF integration on TN across key PQ

measures. Case-1 with scenario 2 did not involve any Q compensation device integrated into the system.

Scenario 1: Techno-economic impact analysis of the ideal base without wake effects and seasonal fluctuations. This scenario discusses the documentation FFCEL has submitted to NEPRA.

Scenario 2: Techno-economic impact analysis of the base scenario with wake effects and no compensation device. This scenario discusses the penalty incurred for failing to adhere to grid codes.

6.2. Case-2: VAR Device-Based Scenario Assessment

Case-2 assesses the Q/VAR compensation device assessment and is comprised of five scenarios, as follows:

Scenario 3: Techno-economic impact analysis considering SVC integration with inter-farm wake effects. This scenario discusses SVCs installed throughout the duration of the plant's useful life (20 years).

Scenario 4: Techno-economic impact analysis considering capacitor bank integration with inter-farm wake effects. This scenario discusses SVCs installed for the first 10 years, and a capacitor bank is replaced beyond the half-life.

Scenario 5: Techno-economic impact analysis considering STATCOM integration with inter-farm wake effects. This scenario discusses SVCs installed for the first 10 years, and a STATCOM is replaced beyond the half-life.

Scenario 6: Techno-economic impact analysis considering SSSC integration with inter-farm wake effects. This scenario discusses SVCs installed for the first 10 years, and an SSSC is replaced beyond the half-life.

Scenario 7: Techno-economic impact analysis considering UPFC integration with inter-farm wake effects. This scenario discusses SVCs installed for the first 10 years, and a UPFC is replaced beyond the half-life.

6.3. Case-3: VAR Devices and Heightening the Hubs-Based Scenario Assessment

Case-3 assesses the Q/VAR compensation device assessment with and increasing the height of the HUB and is comprised of five scenarios, as follows:

Scenario 8: Techno-economic impact analysis considering SVC integration with the heightening effects of the hub. This scenario discusses the SVCs installed throughout the duration of the plant's useful life (20 years) and increasing the height of the HUB beyond the half-life.

Scenario 9: Techno-economic impact analysis considering capacitor bank integration with the heightening effects of the hub. This scenario discusses the SVCs installed for the first 10 years, a capacitor bank being replaced, and increasing the height of the HUB beyond the half-life.

Scenario 10: Techno-economic impact analysis considering STATCOM integration with the heightening effects of the hub. This scenario discusses the SVCs installed for the first 10 years, a STATCOM being replaced, and increasing the height of the HUB beyond the half-life.

Scenario 11: Techno-economic impact analysis considering SSSC integration with the heightening effects of the hub. This scenario discusses the SVCs installed for the first 10 years, an SSSC being replaced, and increasing the height of the HUB beyond the half-life.

Scenario 12: Techno-economic impact analysis considering UPFC integration with the heightening effects of the hub. This scenario discusses the SVCs installed for the first 10 years, a UPFC being replaced, and increasing the height of the HUB beyond the half-life.

6.4. Environmental Analysis

The environmental analysis considers all scenarios to determine the most efficient scenario in terms of environmental and GHG emission reduction.

7. Simulations, Results, and Discussions

7.1. Case-1 Evaluation: Base Case Scenarios Assessment

7.1.1. Case-1, Scenario 1: Proposed by FFCEL to NEPRA

This scenario does not consider the wake effect. This instance is subjected to a techno-economic examination of the determination given to NEPRA to establish a baseline for comparison with the remaining possibilities in this research. FFCEL has acquired 1.5 MW Nordex S77 wind turbines with hub heights of 80 m for their project. Thirty-three of these turbines add up to a total plant capacity of 49.5 MW. The projected energy output is 143.559 GWh with a capacity factor of 33.11%. The local bank's loan is USD 106 million with a ten-year term, and the equity from the entire cost of the project is USD 28 million with a six-year term. The O&M cost is USD 3 million/annum. To compensate for Q, the SCV device has been placed by FFCEL. The payback period for this scenario is calculated to be 5.4 years. The SPP on equity is 6.259 years, which is approximate to the proposed determination. The IRR calculated is 14.45%, and the NPV at the end of the project life is calculated as USD 209,996,976. This scenario's total cash flow is USD 907 million, as shown in Figure 6a.

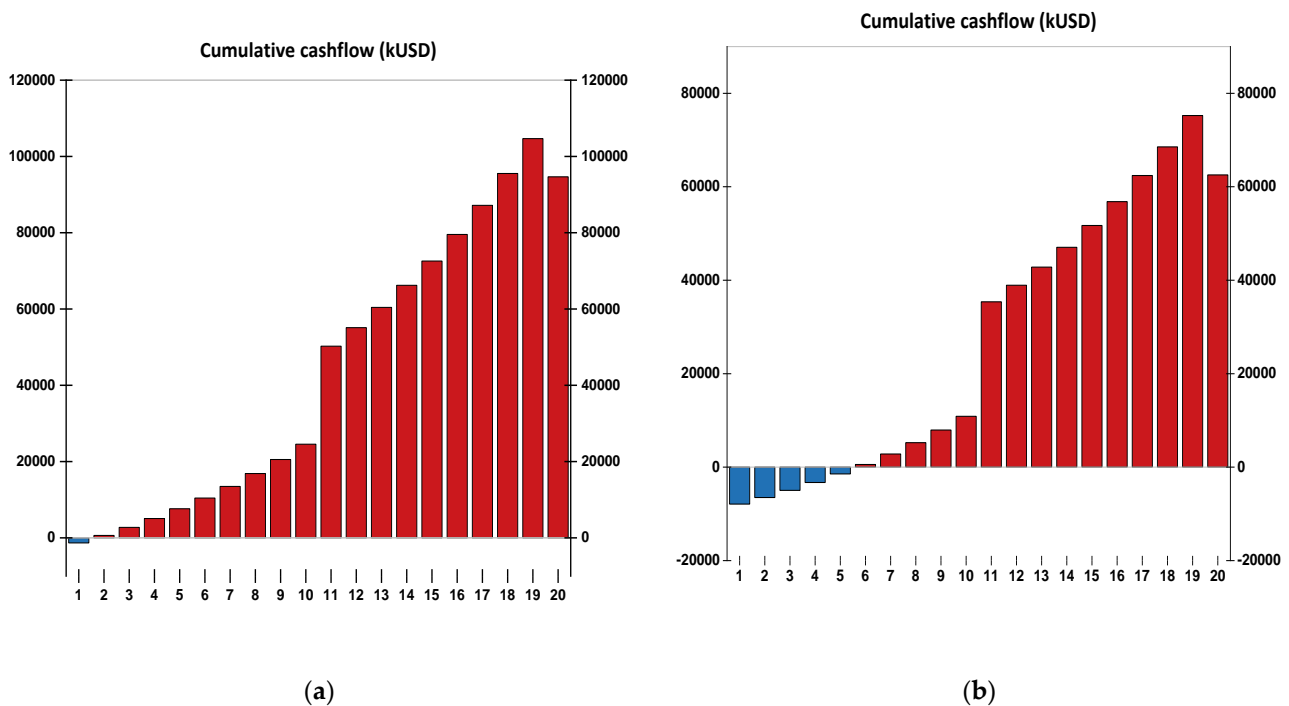


Figure 6. Cumulative cashflows: (a) Case 1 scenario 1, and (b) Case 1 scenario 2.

7.1.2. Case-1, Scenario 2: Without any Compensation Device (Penalty Imposed for Failure to Adhere to Grid Codes)

This scenario considers the wake effects with no compensation devices installed and is compared with scenario 1. Due to wake, the power decreases from 49.50 to 40.45 MW. The voltages (V) at PCC are noted to be 0.9704 pu. The PF retrieve is 0.959, and the Q absorption seems to be 2.748 MVAR. A penalty will be imposed for breaches of the grid codes. The amount of penalty considered in this study is 3% of the revenue earned, according to [78]. For this case, the payback period is 7.2 years, and the SPP on equity is 11 years. This scenario shows up an unacceptable IRR of 7.76%, with an NPV at the end of the project life computed as USD 60,637,276. The net cash flows are USD 584,815,23, as shown in Figure 6b.

7.2. Case-2 VAR Devices Based Scenario Assessment

7.2.1. Case-2, Scenario 3: SVC Installed throughout the Duration of Its Useful Life (20 Years)

This scenario replicates the current state of the wind farm (FFCEL), including wake effects and the SCV employed as a compensating mechanism for a complete life of wind farm, and compares the results to scenario 1. The SVC impact appears to be that we begin noting supplying Q of 23.77 MVAR. At PCC, the voltage computed is 1.028 pu and the PF noted is 0.999. The payback period is increased due to the wake effects and completed in 6.5 years, and SPP on equity is also extended to 9.81 years. The project’s NPV at the end of its life is USD 134,946,432. Net cash flows total USD 677,379,724, as shown in Figure 7a, with an IRR of 10.413%.

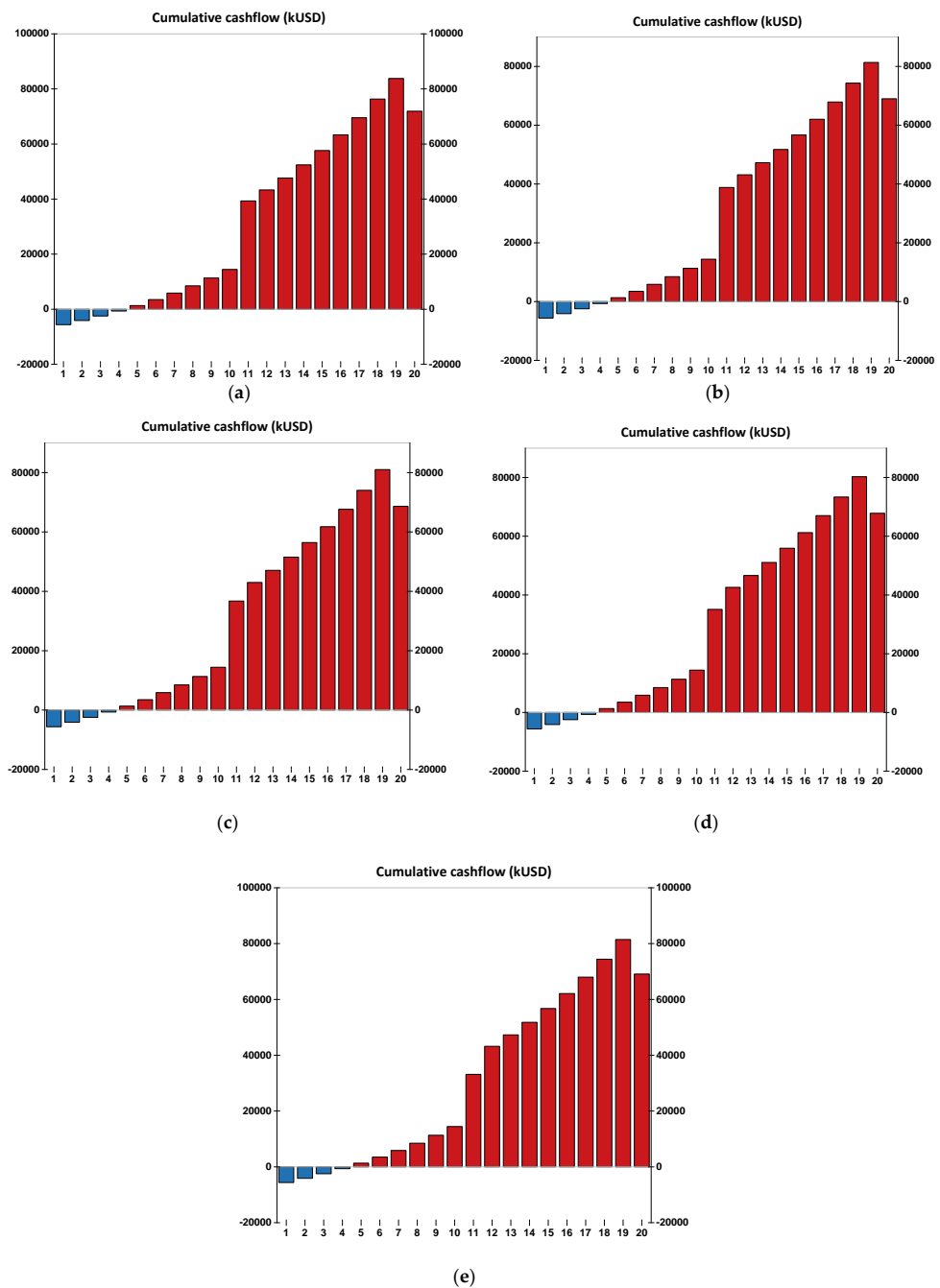


Figure 7. Cumulative cashflows: (a) Case 2 scenario 3; (b) Case 2 scenario 4; (c) Case 2 scenario 5; (d) Case 2 scenario 6; (e) Case 2 scenario 7.

7.2.2. Case-2, Scenario 4: SVC Is Placed for the First 10 Years, and a Capacitor Bank Is Replaced beyond the Half-Life

Scenario 4 employs SVC for the first half of the wind farm's life, i.e., 10 years, with an additional investment made to install a capacitor bank for the remainder of the wind farm's life. This scenario contains a detailed techno-economic analysis of the wind farm's first half-life and remaining life. The change in power after installing the capacitor bank is increased by up to 1.36%, from 40.37 to 40.92. Q seems to change from 23.77 to 23.81 MVAR. The voltage and PF at PCC seem to be the same, i.e., 1.028 and 0.999, respectively. The NPV calculated is USD 136,638,432, which seems increased compared to the current state (scenario 3). The IRR computed is 10.234, with the net cash flow after 20 years being USD 664,404,939.54, as shown in Figure 7b.

7.2.3. Case-2, Scenario 5: SVC Is Placed for the First 10 Years, and a STATCOM Bank Is Replaced beyond the Half-Life

In scenario 5, before the half-life, an SVC is installed and an extra investment for improved power quality and Q compensation STATCOM is made on PCC after the wind farm's half-life. After installing STATCOM, the power output rises by 0.62%, from 40.37 to 40.62. The value of Q appears to decrease from 23.77 to 4.751 MVAR. At PCC, the voltage and PF are predicted to be 1.006 and 0.962, respectively. The NPV after 20 years is calculated to be USD 135,564,320, which seems greater compared to scenario 3 and less than scenario 4. The calculated IRR is 10.144, with a net cash flow of USD 660,043,295.86 after 20 years, as shown in Figure 7c.

7.2.4. Case-2, Scenario 6: SVC Is Placed for the First 10 Years, and an SSSC Bank Is Replaced beyond the Half-Life

Scenario 6 is concerned with SSSC employment after the half-life of a wind farm. After the replacement, P decreases by 1.07%, from 40.37 to 39.94 MW. The value of Q appears to fall from 23.77 to 2.007 MVAR. The voltage remains stable up to 1.004 pu, which is extremely near to the nominal value of 1 pu, and the PF is 0.960. The project's NPV after 20 years will be USD 132,700,992. The computed IRR is 10.202, with a net cash flow of USD 653,238,967.53 after 20 years, as shown in Figure 7d. Because of its network series link, SSSC seems to have a minimal P deficit, implying that it is responsible for the highest P and Q deficit during the wake, making it unsuitable for this situation.

7.2.5. Case-2, Scenario 7: SVC Is Placed for the First 10 Years, and a UPFC Bank Is Replaced beyond the Half-Life

In this scenario, an SVC is placed for the first half of the farm's life, and then a UPFC is deployed throughout the remaining farm life. P seems to grow by 1.6% following the UPFC deployment, from 40.37 to 41.01 MW. Q changes from 23.77 to 3.888 MVAR. The voltage is set to 1.002 pu, which is extremely near to the nominal value of 1 pu. In comparison to other compensating devices, it has the best reaction in terms of maintaining the voltage at PCC at such a close level to its nominal value. The PF is 0.962. In comparison to the current condition (scenario 3), a significant change in NPV appears towards the end of 20 years, i.e., USD 137,168,144. The IRR is 10.094%, with a net cash flow of USD 659,411,175.56, as shown in Figure 7e.

7.3. Case-3: VAR Devices and Heightening the Hubs-Based Scenario Assessment

7.3.1. Case-3, Scenario 8: SVC Installed throughout the Duration of Its Useful Life (20 Years), and HUB Height Increases beyond the Half-Life

Scenario 8 presents the employment of an SVC for the complete life of the wind farm, and additional investment is made after the half-life of a plant to increase the HUB height. As the current state is facing 32% of wake, according to [21], by raising the HUB height from 80 to 100 m, the wake is reduced to 25%. After the heightening, the power appears to increase by 5.8%, from 40.37 to 42.72 MW. An increase in power results in improvements in energy generation from 116 to 123 MWh, and, as a result, the net cash flow at the end

of 20 years is calculated to be USD 656,764,248.39, as shown in Figure 8a, with an IRR of 10.157%. The NPV of a project after 20 years is computed to be USD 144,146,864.

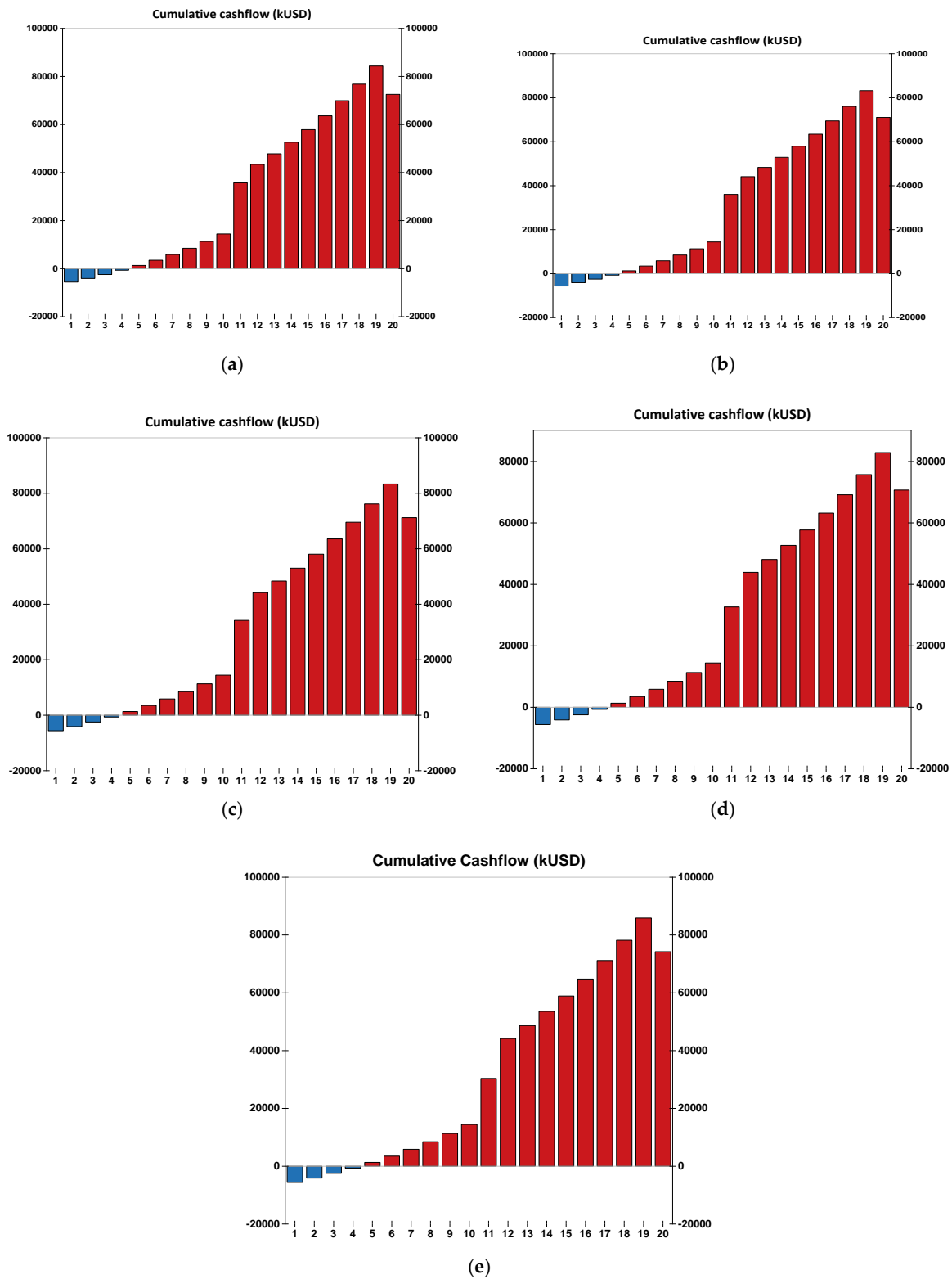


Figure 8. Cumulative cashflows: (a) Case 3 scenario 8; (b) Case 3 scenario 9; (c) Case 3 scenario 10; (d) Case 3 scenario 11; (e) Case 3 scenario 12.

7.3.2. Case-3, Scenario 9: SVC Is Placed for the First 10 Years, Capacitor Bank Is Replaced, and HUB Height Increases beyond the Half-Life

Scenario 9 depicts the use of an SVC for the first half-life of a wind farm, followed by a further expenditure to raise the HUB height and replace the SVC with a capacitor bank after the half-life of the plant. Wake reduces leads to a rise in power, which results in a net cash flow of USD 674,858,459.04, as shown in Figure 8b, with an IRR of 10.360%. After 20 years, the NPV of the project is calculated to be USD 143,954,512.

7.3.3. Case-3, Scenario 10: SVC Is Placed for the First 10 Years, STATCOM Is Replaced, and HUB Height Increases beyond the Half-Life

Scenario 10 depicts the use of a STATCOM and the raising of the HUB height after the wind farm's half-life. The additional investment improves PQ and helps to improve the power quality of the system up to a nominal value. The P improves from 40.37 to 42.77 MW, with cash flows of USD 673,821,360.14 at the end of 20 years, as shown in Figure 8c. The NPV of a project in this scenario is determined to be USD 144,368,560, with an IRR of 10.324%. The performance of the wind farm is improved by a combination of rising the hub height and the employment of STATCOM, which provide flexibility in balancing Q flows and help keep the voltage stable, as mentioned in scenario 5.

7.3.4. Case-3, Scenario 11: SVC Is Placed for the First 10 Years, SSSC Is Replaced, and HUB Height Increases beyond the Half-Life

Scenario 11 delineates the employment of SVC for the first half-life of the wind farm, and additional investment is carried out in the employment of SSSC and raising the hub height up to 100 m. The increase in hub height improves P deficits from 40.37 to 42.34 MW, but, as mentioned in scenario 6, because of the network series link, the SSSC is inappropriate as compensation for Q during the wake situation. The NPV after additional investment at the end of 20 years is USD 142,700,944, with an IRR of 10.236%. The net cash flow at the end of the project life will be USD 669,044,194.47, as shown in Figure 8d. The NPV of the project and the cash outflows seem to be poor compared to other scenarios with such investment.

7.3.5. Case-3, Scenario 12: SVC Is Placed for the First 10 Years, UPFC Is Replaced, and HUB Height Increases beyond the Half-Life

Scenario 12 considers the employment of a UPFC and enhancing the hub height after the half-life of a wind farm; an SVC is considered employed in the first half-life. The P deficit improves from 40.37 to 42.78 MW, which yields better cash flows at the end of 20 years compared to other scenarios of the study, i.e., USD 682,223,689.44, as shown in Figure 8e. The NPV calculated is USD 144,419,296, with an IRR of 10.383%. In our research, the UPFC performs better in terms of improving PQ indicators and PS parameters under the influence of wake; from an investment and economic perspective, the UPFC performs well in comparison to other compensation devices. The revenue of generation from LSWFs in all cases across the life cycle cost is separately shown in Figure A1 in Appendix A.

7.4. CO₂ Reduction and Environmental Assessment

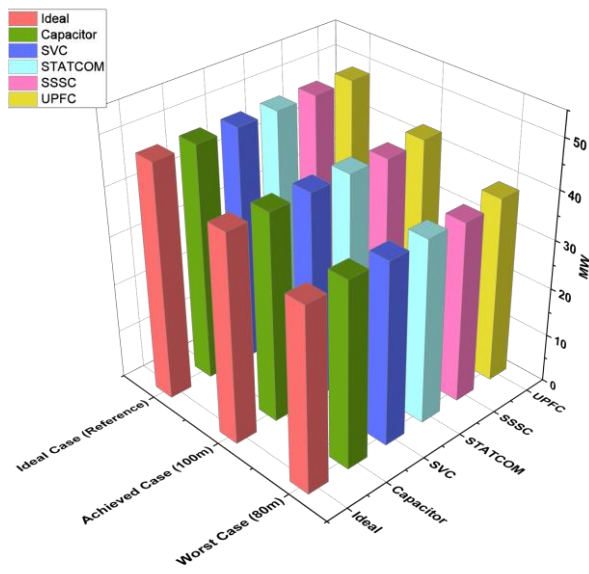
All scenarios are examined in this assessment for the best possible environmental scenario. In this research, environmental analysis is performed using RET screen software. Scenario 1 is used as a baseline against which subsequent scenarios are compared with the suggested scenario; the FFCEL wind farm may assist in eliminating up to 60,455.6 tCO₂ yearly. However, the energy imbalance caused by the wake did not allow for this CO₂ decrease. Scenario 3 corresponds to the current state of the FFCEL wind farm, which has a deficit of 22.55%, or 11.44 tCO₂ yearly. This shortfall is offset in some way by the renovation of wind farms.

8. Results Validation

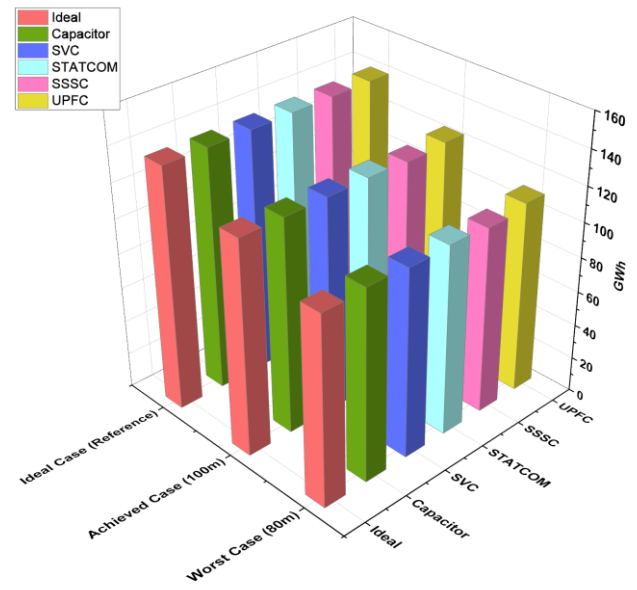
8.1. Comparison between Proposed Cases with a Base Case

When DFIGs were introduced, P increased, as did Q supply through the turbines. The P and Q outputs increased in proportion to the wind speed, as shown in Table 3. Previous research in [21] provided a method for reducing the effect of wake by raising the hub height of WTs. During wakes, compensation devices play an essential role in guaranteeing the supply of Q to wind farms, leading to the strengthening and stabilization of PS. Every Q compensating device has its own set of advantages and disadvantages. By raising the hub height from 80 to 100 m, a hindrance from upstream wind turbines can be eliminated, and more wind potential is accessible to wind turbines for greater P extraction. After extending the hub height to 20 m, Table 4 may be used to compare PS parameters. According to the case study [21], the considered wake is 32% and may be decreased to 25% if a height of 100 m is attained. The wind speed was assumed to remain constant at 15 m/s in the referenced case study [21]; therefore, we used that value for our suggested base case scenario. We examined an average wind speed of 11 m/s by raising the height and a current instance with a wind speed of 10 m/s. To get the greatest feasible combination solution, these three wind scenarios are evaluated using a capacitor bank and numerous facts devices. In our research study, we used this idea for P and Q repowering. As shown in Figure 9c, capacitor banks and SVCs exhibit the highest reactive power supply due to the inflexibility of these devices, which provide the maximum of their values, rendering the system susceptible to swells and severe transients. Figure 10c shows that the capacitor bank generates harmonic resonance and does not offer flexibility in its voltage-maintenance function, which may occasionally exacerbate the existing over- and under-voltage conditions. STATCOM offers better dampening and higher power quality than the SVC. The SSSC is good at maintaining power flow. Figure 9a shows the SVC has the greatest P deficit and the lowest is from the UPFC. Figure 9c shows STATCOM had the largest Q deficit while the UPFC had the lowest. Figure 10c shows that the UPFC keeps the voltage and frequency as close to the nominal levels as possible. Figure 10b reveals that the UPFC offers maximum power handling capabilities by changing the network's impedance as little as possible. The UPFC also maintains the power factor within acceptable limits, as shown in Figure 10a. A decrease in P and Q deficits may be found by comparing Table 3. CO₂ reduction comparison of different cases can be shown in Figure 9h. The carbon footprints on different wind speeds with different compensation devices are shown in Table 5.

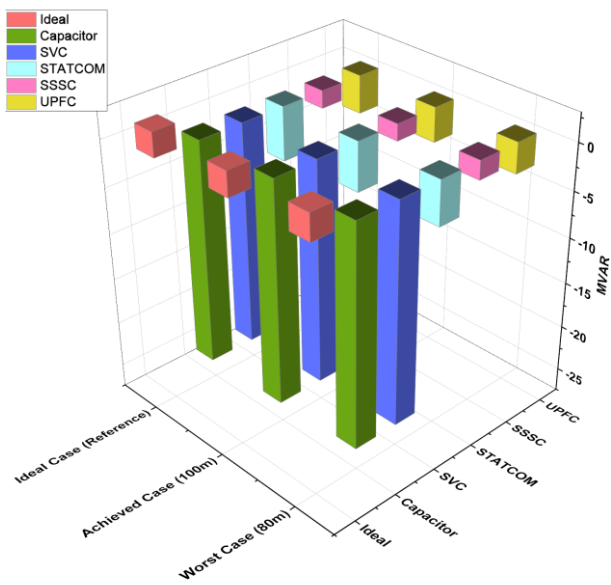
The P and Q deficit by raising hub height from 80 to 100 m may be seen in Figure 9a,c. The improvement in energy can be seen in Figure 9b. When we compare the revenue at the end of the wind farm's life, as shown in Figure 9g, investing in reducing wake is advantageous for such projects with fast SPP. The UPFC is a device that provides reactive power assistance to the PS to strengthen and stabilize it as well as to maintain PS parameters in the most cost-effective manner possible in comparison to other compensating devices with a wake perspective, as shown in Table 6. We deemed UPFC the best compensating device based on these criteria.



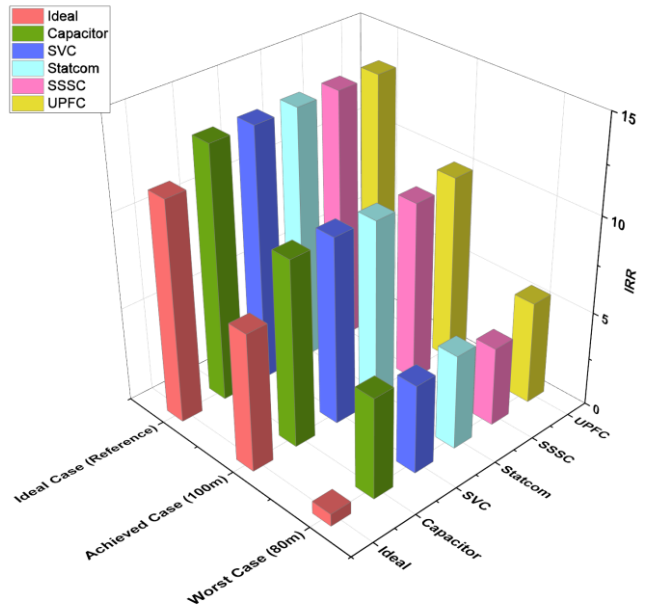
(a)



(b)

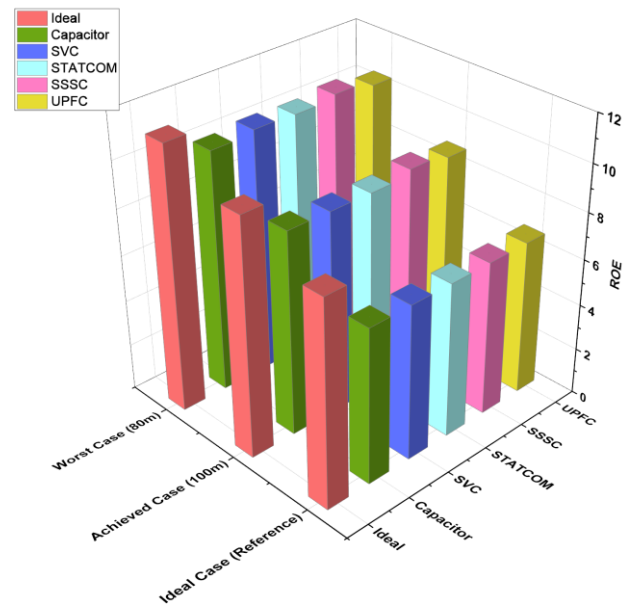
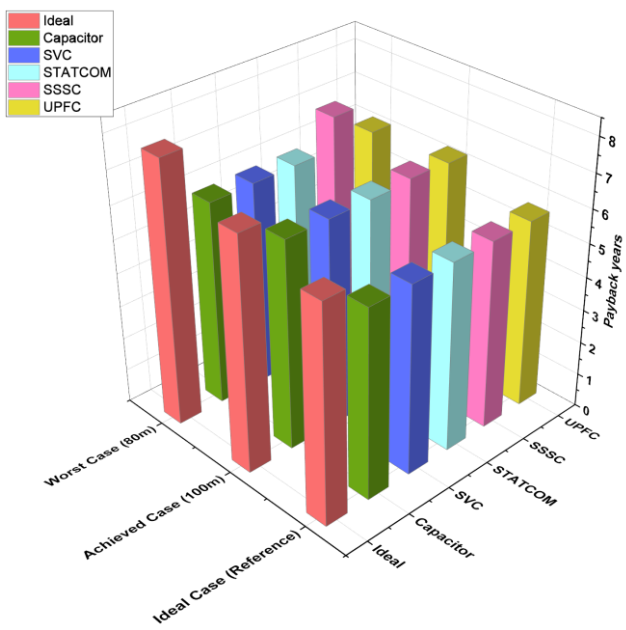


(c)



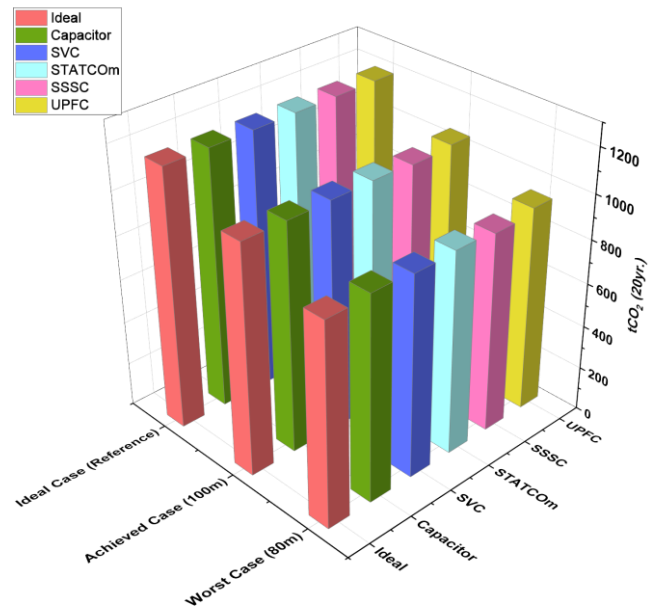
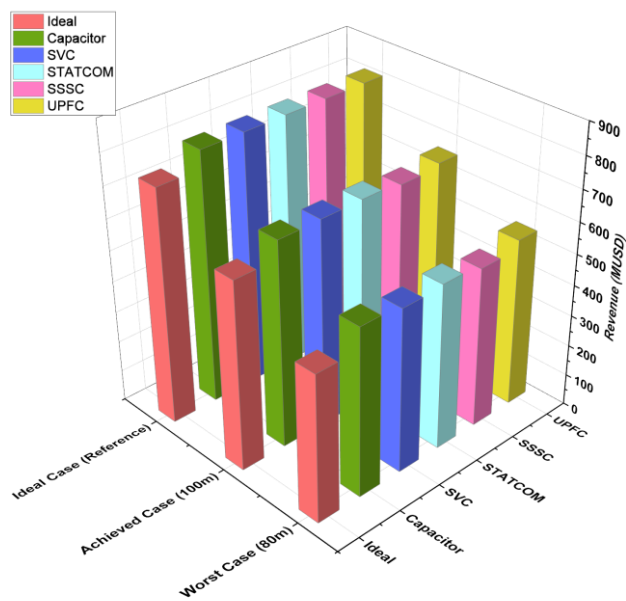
(d)

Figure 9. Cont.



(e)

(f)



(g)

(h)

Figure 9. (a) Power (MW); (b) energy (GWh); (c) MVAR; (d) SPP (years); (e) IRR; (f) ROE; (g) revenue; (h) tCO₂.

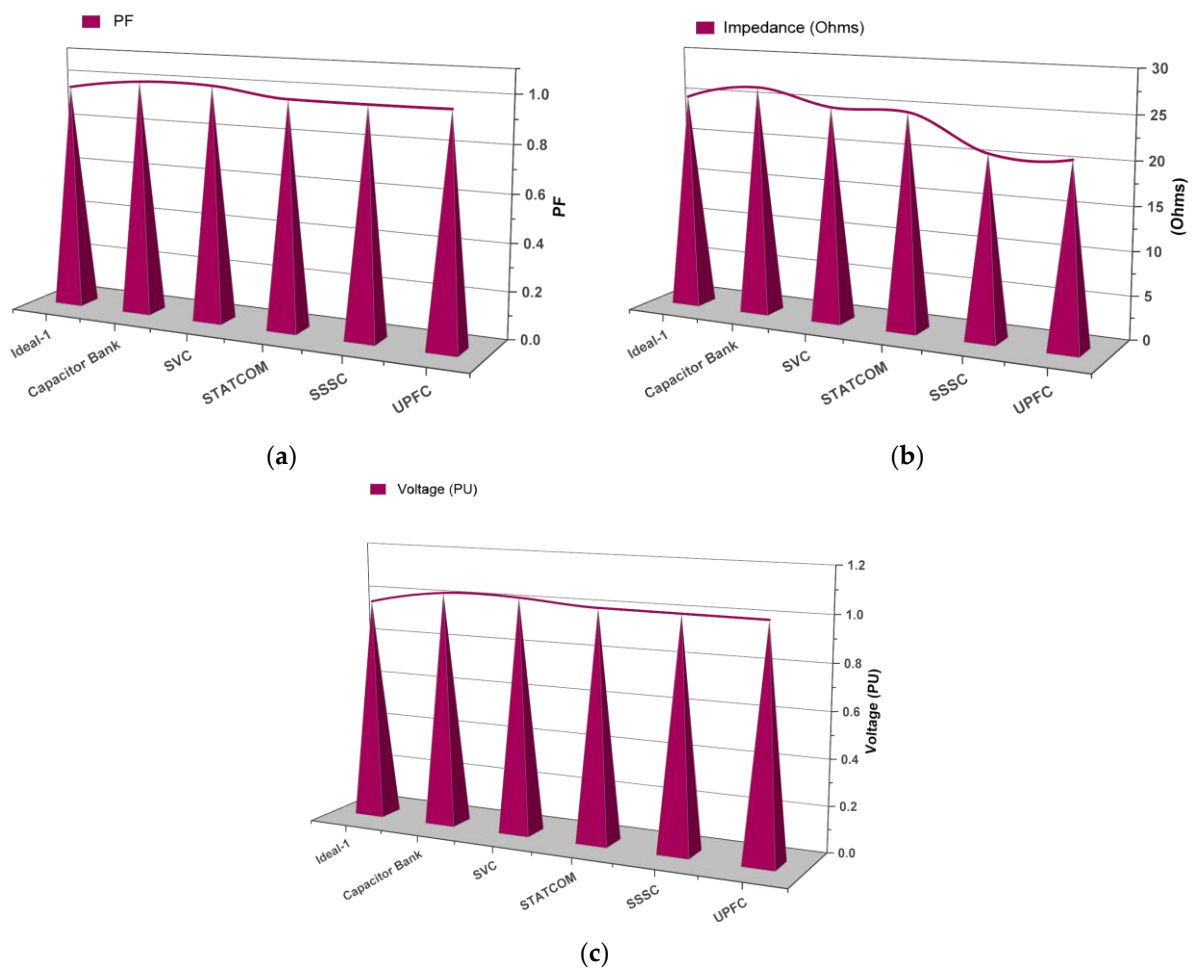


Figure 10. (a) P.F.; (b) impedance; (c) voltage (pu).

Table 3. P and Q comparison of different scenarios.

Wind Speed	Devices	Power (MW)	Reactive Power Q (MVAR)	Energy (KWh)
15 (m/s) [21]	Ideal	48.28	2.574	139,567,824
	Capacitor	48.25	-24.33	139,481,100
	SVC	48.25	-24.33	139,481,100
	Statcom	48.29	-5.813	139,596,732
	SSSC	48.3	-1.887	139,625,640
	UPFC	48.31	-4.109	139,654,548
11 (m/s) At 100 m HUB height	Ideal	42.7	2.617	123,437,160
	Capacitor	42.66	-24.08	123,321,528
	SVC	42.72	-24.08	123,494,976
	Statcom	42.77	-5.283	123,639,516
	SSSC	42.34	-1.797	122,396,472
	UPFC	42.78	-3.713	123,668,424
10 (m/s) At 80 m HUB height	Ideal	37.63	2.749	108,780,804
	Capacitor	38.07	-23.76	110,052,756
	SVC	37.55	-23.77	108,549,540
	Statcom	37.79	-4.746	109,243,332
	SSSC	37.16	-2.007	107,422,128
	UPFC	38.15	-3.28	110,284,020

Table 4. PS comparison of various scenarios.

Scenario #:	P(MW) with Wake at Hub Height = 80 m	P(MW) with Wake at Hub Height = 100 m	V (pu)	Transient F (Hz)	Impedance (Ohms)	PF
Ideal	37.63	42.70	0.9704	49.36–50.89	24.96	0.959
Capacitor Bank	38.07	42.66	1.028	49.55–50.41	26.53	0.999
SVC	37.55	42.72	1.028	49.75–50.24	24.76	0.999
STATCOM	37.79	42.77	1.006	49.76–50.26	24.76	0.962
SSSC	37.16	42.34	1.004	49.67–50.75	20.83	0.960
UPFC	38.15	42.78	1.002	49.88–50.17	20.83	0.962

Table 5. Emissions details.

Wind Speed	Devices	Net Annual GHG Emission Reduction tCO ₂	GHG Emission Reduction tCO ₂ (20 Y)
15 (ms-1)	Ideal	58,758.0539	1,175,161.078
	Capacitor	58,721.5431	1,174,430.862
	SVC	58,721.5431	1,174,430.862
	Statcom	58,770.22417	1,175,404.483
	SSSC	58,782.39444	1,175,647.889
	UPFC	58,794.56471	1,175,891.294
10.714 (ms-1) At 100 m HUB height	Ideal	51,967.04436	1,039,340.887
	Capacitor	51,918.36329	1,038,367.266
	SVC	51,991.3849	1,039,827.698
	Statcom	52,052.23624	1,041,044.725
	SSSC	51,528.91471	1,030,578.294
	UPFC	52,064.4065	1,041,288.13
10.232 (ms-1) At 80 m HUB height	Ideal	45,796.71848	915,934.3697
	Capacitor	46,332.21028	926,644.2055
	SVC	45,699.35634	913,987.1268
	Statcom	45,991.44277	919,828.8554
	SSSC	45,224.71589	904,494.3178
	UPFC	46,429.57242	928,591.4484

Table 6. Economical details.

Wind Speed	Devices	SPP (Year)	ROE (Year)	IRR	Cashflows
Wind speed 15 (ms-1)	Ideal	6.44	8.860	11.617	754,310,745.87
	Capacitor	5.639	6.714	13.335	810,062,392.75
	SVC	5.639	6.714	13.335	810,062,392.75
	Statcom	5.633	6.698	13.356	811,122,044.39
	SSSC	5.632	6.694	13.361	811,386,957.30
	UPFC	5.631	6.690	13.366	811,651,870.21
Wind speed 10.714 (ms-1) At 100 m HUB height	Ideal	6.971	10.219	7.228	606,489,342.28
	Capacitor	6.232	8.7944	9.774	661,976,076.25
	SVC	6.222	8.763	9.821	663,565,553.71
	Statcom	6.215	8.737	9.860	664,890,118.26
	SSSC	6.281	8.966	9.519	653,498,863.14
	UPFC	6.213	8.731	9.868	665,155,031.17
Wind speed 10.232 (ms-1) At 80 m HUB height	Ideal	7.862	11.416	0.652	472,178,497.09
	Capacitor	6.1044	10.409	5.303	540,381,050.72
	SVC	6.1151	10.546	4.657	526,605,579.42
	Statcom	6.1101	10.482	4.961	532,963,489.25
	SSSC	7.032	10.652	4.151	516,273,975.94
	UPFC	6.1028	10.388	5.399	542,500,354.00

8.2. Comparative Analysis of Result via Proposed Methodology

In the proposed methodology, the refurbishment after the half-life is discussed because, currently, the wind farm has covered its almost half-life as the life of FFCEL is 20 years. If the comparison is made among all proposed cases, we find that scenario 12 is probably the best. The investment after half-life for all scenarios is shown in Table 7. The payback period of scenarios 1, 2, and 3 is shown in Figure 11a. From Table 8, it seems that the payback period of the proposed case is 5.4 years without considering wake. The payback period of the scenario in which wake is considered and without any compensation device is 7.2 years, and the payback period of the scenario considering wake and compensation device is 6.5 years.

The power deficit is shown in Figure 11b.

Table 9 shows the power and energy deficit for the first and second half-life of the wind farm life. The NPV and revenue at the end of farm life are shown in Figure 11c. Figure 11d shows the IRR comparison of all scenarios presented in this study. Table 9 shows that if we compare the NPV and net cash flows of all scenarios, the best result will be obtained by scenario 12 in which investment is made for the UPFC to be installed with the increase in height after half-life.

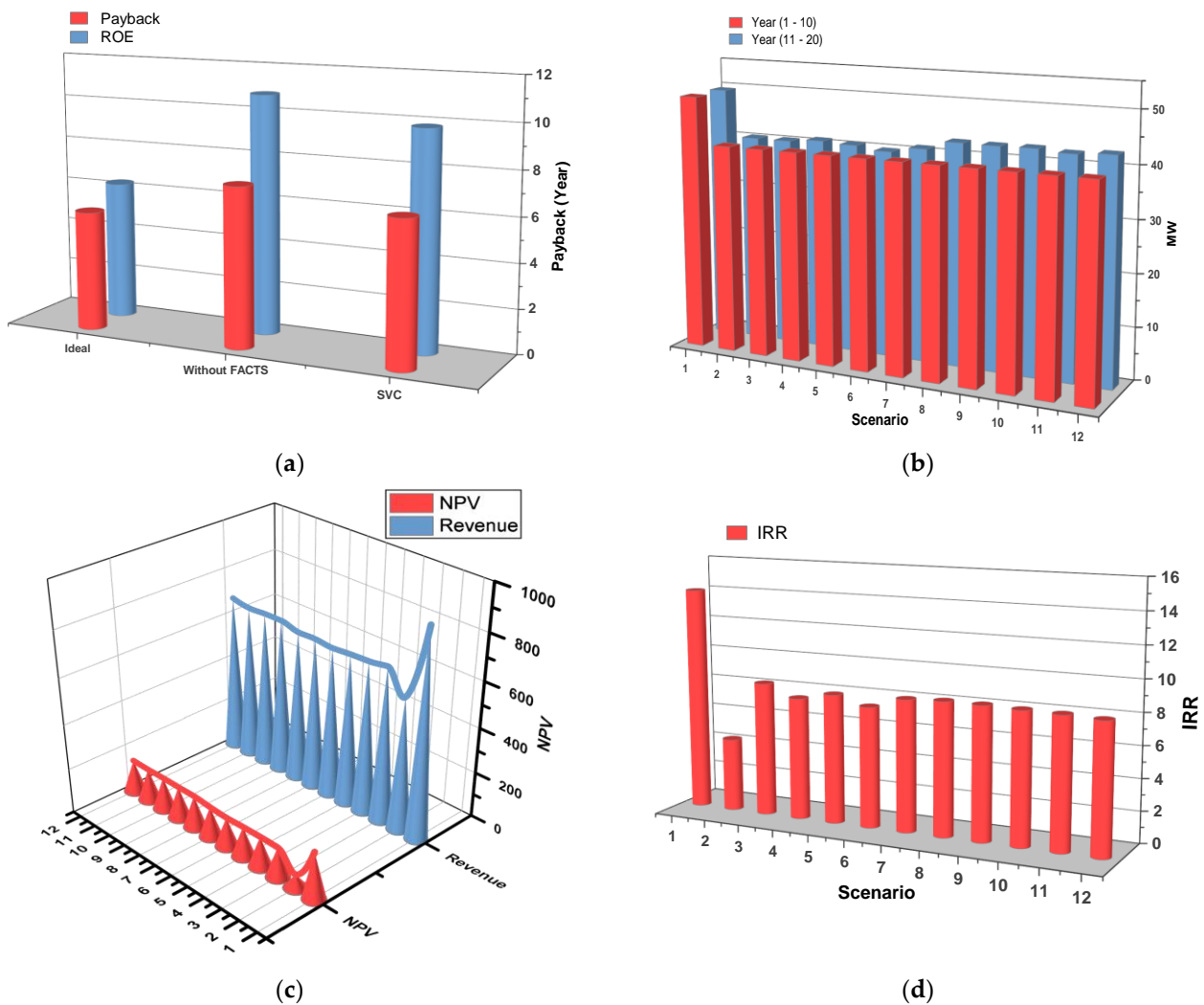


Figure 11. Cont.

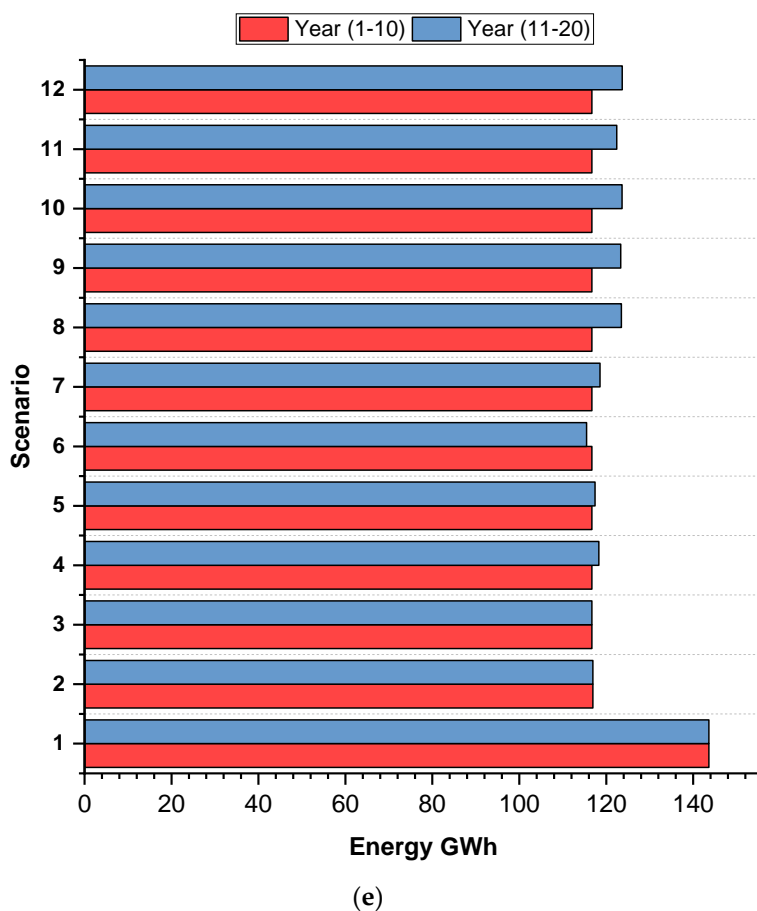


Figure 11. (a) SPP and ROE; (b) before and after refurbishment, power (MW) variation among scenarios; (c) revenue and NPV variation among scenarios; (d) IRR variations among scenarios; (e) before and after refurbishment, energy (GWh) variation among scenarios.

Wind energy plays a significant part in reducing carbon footprints in the environment. Traditional power plants have long been a key contributor to climate change and acid rain due to high levels of energy consumption and greenhouse gas (GHG) emissions. For a clean and healthy ecosystem, GHG emissions must be appropriately removed from the atmosphere since they are the major cause of global warming, which affects millions of people worldwide. With an annual producing capacity of 143 GWh and a 20-year operation lifetime, the carbon emissions reduction attributable to the FFCEL wind farm over its entire life cycle is 1,209,112 tCO₂. Due to energy shortages caused by the wake effect, conventional power plants are required, resulting in an 18.57% rise in carbon footprints, as seen in Table 10. The refurbishment made in this study helps to overcome these deficits. Figure 12 shows the detailed reduction in CO₂ before and after the refurbishment of wind plants.

Table 7. Investment details.

	Scenario	USD
Scenario 1	Proposed by FFCEL to NEPRA	-
Scenario 2	Without any compensation device (penalty imposed for failure to adhere to grid codes)	Penalty
Scenario 3	SVC installed throughout the duration of its useful life (20 years)	-
Scenario 4	SVC is placed for the first 10 years, and a capacitor bank is replaced beyond the half-life.	500,000
Scenario 5	SVC is placed for the first 10 years, and a STATCOM bank is replaced beyond the half-life.	2,177,437.5
Scenario 6	SVC is placed for the first 10 years, and an SSSC bank is replaced beyond the half-life.	3,299,562.5
Scenario 7	SVC is placed for the first 10 years, and a UPFC bank is replaced beyond the half-life.	5,477,000
Scenario 8	SVC installed throughout the duration of its useful life (20 years) and HUB height	3,178,735.84
Scenario 9	SVC is placed for the first 10 years, the capacitor bank is replaced, and HUB height increases beyond the half-life.	3,678,735.84
Scenario 10	SVC is placed for the first 10 years, STATCOM is replaced, and HUB height increases beyond the half-life.	5,356,173.34
Scenario 11	SVC is placed for the first 10 years, SSSC is replaced, and HUB height increases beyond the half-life.	6,478,298.34
Scenario 12	SVC is placed for the first 10 years, UPFC is replaced, and HUB height increases beyond the half-life.	8,655,735.84

Table 8. Economical details.

Case	Payback (Year)	SPP (Year)	IRR%	Revenue (End 20 Y)	NPV
Scenario 1	5.4	6.259	14.45	907,017,158.03	209,996,976
Scenario 2	7.2	10.8	7.76	584,815,234.33	60,637,276
Scenario 3	6.5	9.81	10.413	677,379,724.04	134,946,432
Scenario 4	6.5	9.81	10.234	664,404,939.54	136,638,432
Scenario 5	6.5	9.81	10.144	660,043,295.86	135,564,320
Scenario 6	6.5	9.81	10.202	653,238,967.53	132,700,992
Scenario 7	6.5	9.81	10.094	659,411,175.56	137,168,144
Scenario 8	6.5	9.81	10.157	656,764,248.39	144,146,864
Scenario 9	6.5	9.81	10.360	674,858,459.04	143,954,512
Scenario 10	6.5	9.81	10.324	673,821,360.14	144,368,560
Scenario 11	6.5	9.81	10.236	669,044,194.47	142,700,944
Scenario 12	6.5	9.81	10.383	682,223,689.44	144,419,296

Table 9. Power and energy comparisons.

Cases	Power (MW)		Energy (KWh)	
	(1–10) Years	(11–20) Years	(1–10) Years	(11–20) Years
Scenario 1	49.5	49.5	143,600,000	143,600,000
Scenario 2	40.45	40.37	116,932,860	116,932,860
Scenario 3	40.37	40.37	116,701,596	116,701,596
Scenario 4	40.37	40.92	116,701,596	118,291,536
Scenario 5	40.37	40.62	116,701,596	117,424,296
Scenario 6	40.37	39.94	116,701,596	115,458,552
Scenario 7	40.37	41.01	116,701,596	118,551,708
Scenario 8	40.37	42.72	116,701,596	123,494,976
Scenario 9	40.37	42.66	116,701,596	123,321,528
Scenario 10	40.37	42.77	116,701,596	123,639,516
Scenario 11	40.37	42.34	116,701,596	122,396,472
Scenario 12	40.37	42.78	116,701,596	123,668,424

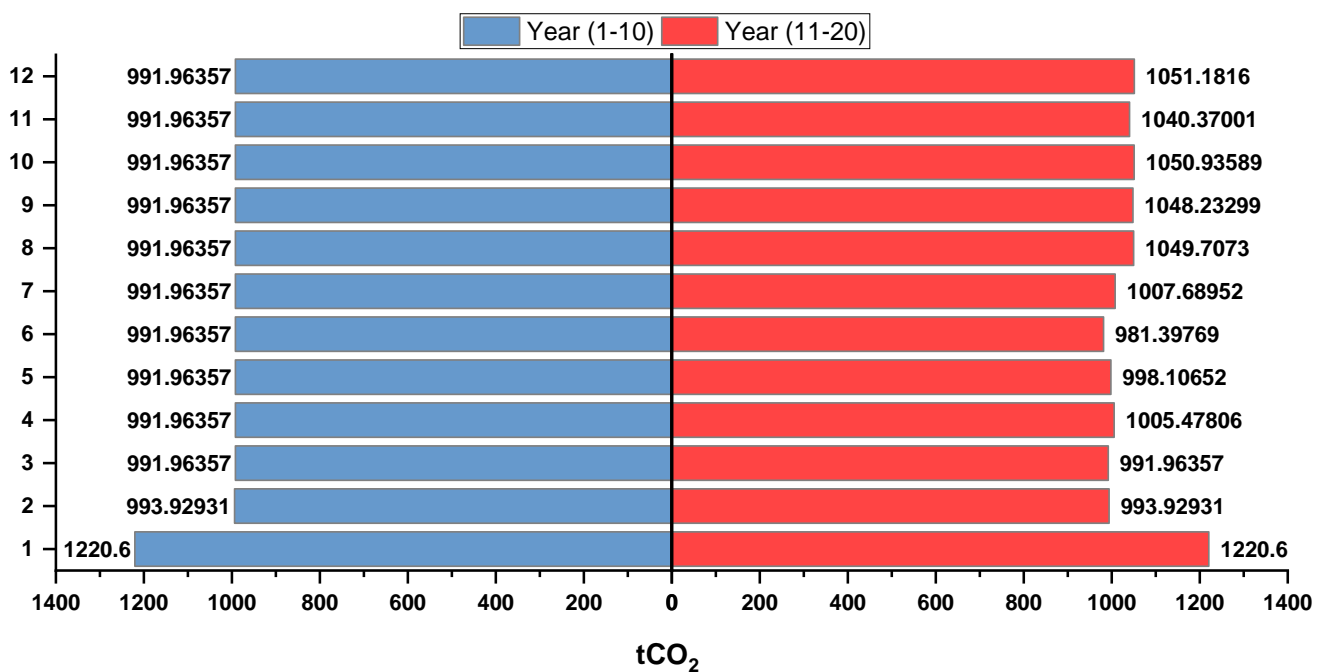
**Figure 12.** Refurbishment results in a decrease in CO₂.

Table 10. Emissions details.

Cases	Net Annual GHG Emission Reduction tCO ₂		GHG Emission Reduction tCO ₂ (20 Y)	
	(1–10) Years	(11–20) Years	(1–10) Years	(11–20) Years
Scenario 1	60,455.6	60,455.6	604,556	604,556
Scenario 2	49,228.73	49,228.73	492,287.3	492,287.3
Scenario 3	49,131.37	49,131.37	491,313.7	491,313.7
Scenario 4	49,131.37	49,800.74	491,313.7	498,007.4
Scenario 5	49,131.37	49,435.63	491,313.7	494,356.3
Scenario 6	49,131.37	48,608.05	491,313.7	486,080.5
Scenario 7	49,131.37	49,910.27	491,313.7	499,102.7
Scenario 8	49,131.37	51,991.38	491,313.7	519,913.8
Scenario 9	49,131.37	51,918.36	491,313.7	519,183.6
Scenario 10	49,131.37	52,052.24	491,313.7	520,522.4
Scenario 11	49,131.37	51,528.91	491,313.7	515,289.1
Scenario 12	49,131.37	52,064.41	491,313.7	520,644.1

9. Conclusions

MATLAB and SAM software is used to perform a comparative study of the concerns linked to LSWFs in a larger context for Pakistan. A complete technical, economic, and environmental study has been determined based on the energy deficit created by the wake effect power pumped into the grid, which is evaluated to imitate real-time circumstances, payback period, and GHG emission reduction. The wake causes a considerable active power loss as well as enhanced Q absorption. For a maximum wake of 32%, FFCEL had a P deficit of 10.65 MW and a Q deficit of +0.174 MVAR owing to wake impact. Furthermore, confirmation of the simulation findings with real FFCEL to NEPRA determinations reveals that the actual data closely match the simulation results.

A specific case study was conducted in which ideal scenario 1 was compared to both Case-2 and Case-3 eventualities. We conducted a performance investigation with several compensation devices to determine the optimal compensation device for enhancing PQ and PS parameters with and without repowering the WF during the wake while raising the WT hub height from 80 to 100 m. A significant quantity of P repowering was found at the highest recuperation of deficiencies, owing to a wake of up to 48%. Our primary goal was to create a device that aids in Q repowering while maintaining V, F, Z, and PF at PCC at the closest nominal number. It is determined that among the compensating devices considered, the UPFC is the most cost-effective and optimal for Q repowering while retaining PS parameters at PCC. As a result, the UPFC kept V up to 1.002 pu, suppressing frequency transients in the 49.88–50.17 Hz region and preventing any resonance while keeping the power factor within acceptable limits.

According to our research, scenario 12 has the largest yearly generation after repowering and the shortest payback time, followed by scenarios 10 and 7. In contrast, scenario 6 has the worst performance, with the lowest yearly generation and the longest payback time after repowering. The study results demonstrate that the proposed scenarios for the renovation of wake-affected WFs linked to a weak grid are possible. Furthermore, repowering a planned system results in a large decrease in CO₂ emissions, which contributes to a greener environment. The research described in this paper will aid policymakers and financiers in finding appropriate repowering approaches for maximizing the return on investment in large-scale projects in Pakistan's industrial sector.

Author Contributions: Conceptualization, S.A.A.K., F.F.A. and Z.A.K.; methodology, S.A.A.K., Z.A.K. and M.A.; software, R.Z.B.; validation, R.Z.B., S.A.A.K. and Z.A.K.; formal analysis, R.Z.B., M.I. and A.A.; investigation, R.Z.B.; resources, Z.A.K., M.A. and A.A.; data curation, R.Z.B. and A.A.; writing—original draft preparation, R.Z.B. and S.A.A.K.; writing—review and editing, Z.A.K., M.A., M.I., F.F.A. and A.A.; visualization, R.Z.B.; supervision, S.A.A.K. and Z.A.K.; project administration, S.A.A.K., M.I. and A.A.; funding acquisition, M.A., F.F.A. and A.A. All authors have read and agreed to the published version of the manuscript.

Funding: This research was funded by the Deputyship for Research & Innovation, Ministry of Education in Saudi Arabia, through project number IFP2021-081.

Institutional Review Board Statement: Not applicable.

Informed Consent Statement: Not applicable.

Data Availability Statement: Not applicable.

Acknowledgments: The researcher(s) would like to thank the Deanship of Scientific Research, Shaqra University, for funding the publication of this project.

Conflicts of Interest: The authors declare no conflict of interest.

Appendix A

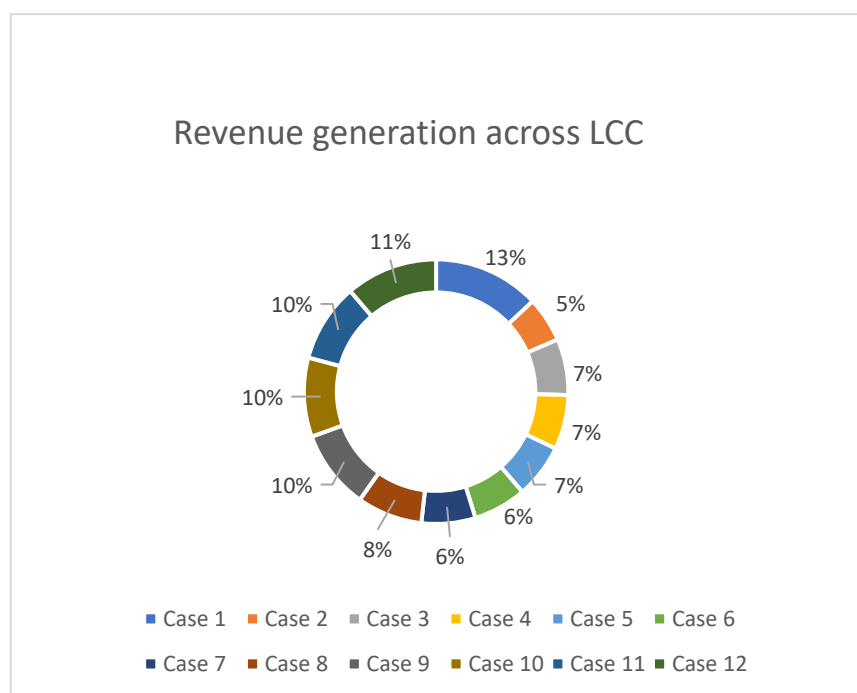


Figure A1. Revenue generation in all cases across the life cycle cost.

References

1. Al-Ghussain, L.; Samu, R.; Taylan, O.; Fahrioglu, M. Techno-Economic Comparative Analysis of Renewable Energy Systems: Case Study in Zimbabwe. *Inventions* **2020**, *5*, 27. [CrossRef]
2. Abdin, Z.; Mérida, W. Hybrid energy systems for off-grid power supply and hydrogen production based on renewable energy: A techno-economic analysis. *Energy Convers. Manag.* **2019**, *196*, 1068–1079. [CrossRef]
3. Yan, J.; Ouyang, T. Advanced wind power prediction based on data-driven error correction. *Energy Convers. Manag.* **2019**, *180*, 302–311. [CrossRef]
4. Renewable Capacity Highlights Renewable Generation Capacity by Energy Source. Available online: www.irena.org/publications (accessed on 15 September 2021).
5. Rahimi, E.; Rabiee, A.; Aghaei, J.; Muttaqi, K.M.; Esmael Nezhad, A. On the management of wind power intermittency. *Renew. Sustain. Energy Rev.* **2013**, *28*, 643–653. [CrossRef]

6. Rona, B.; Güler, Ö. Power system integration of wind farms and analysis of grid code requirements. *Renew. Sustain. Energy Rev.* **2015**, *49*, 100–107. [[CrossRef](#)]
7. Wind Energy Comes of Age—Paul Gipe—Google Books. Available online: https://books.google.com.pk/books?hl=en&lr=&id=8itBNxBL4igC&oi=fnd&pg=PR13&ots=HPrxBnHxgT&sig=SWeCcG6C4U7jvrzj1Ql1_k0AT3w&redir_esc=y#v=onepage&q&f=false (accessed on 17 September 2021).
8. Manwell, J.F.; McGowan, J.G.; Rogers, A.L. *Wind Energy Explained: Theory, Design and Application*. Available online: https://books.google.com.pk/books?hl=en&lr=&id=roaTx_Of0vAC&oi=fnd&pg=PR5&ots=O4TzVvfMY9&sig=A0OawDmM59LN8AIE9g4kV9KywMU&redir_esc=y#v=onepage&q&f=false (accessed on 17 September 2021).
9. Global Wind Atlas. Available online: <https://globalwindatlas.info/> (accessed on 17 September 2021).
10. Adelaja, A.; McKeown, C.; Calnin, B.; Hailu, Y. Assessing offshore wind potential. *Energy Policy* **2012**, *42*, 191–200. [[CrossRef](#)]
11. Komusanac, I.; Fraile, D.; Brindley, G. Wind energy in Europe in 2019—Trends and statistics. Available online: <https://windeurope.org/intelligence-platform/product/wind-energy-in-europe-in-2019-trends-and-statistics/> (accessed on 17 September 2021).
12. Ramírez, L.; Fraile, D.; Brindley, G. Offshore wind in Europe: Key trends and statistics 2019. 2020. Available online: <http://imis.nioz.nl/imis.php?module=ref&refid=321467> (accessed on 17 September 2021).
13. Huang, Y.W.; Kittner, N.; Kammen, D.M. ASEAN grid flexibility: Preparedness for grid integration of renewable energy. *Energy Policy* **2019**, *128*, 711–726. [[CrossRef](#)]
14. MF, H.; SK, L.; JO, D. Wind farm power optimization through wake steering. *Proc. Natl. Acad. Sci. USA* **2019**, *116*, 14495–14500. [[CrossRef](#)]
15. Topham, E.; McMillan, D. Sustainable decommissioning of an offshore wind farm. *Renew. Energy* **2017**, *102*, 470–480. [[CrossRef](#)]
16. Staffell, I.; Green, R. How does wind farm performance decline with age? *Renew. Energy* **2014**, *66*, 775–786. [[CrossRef](#)]
17. Castro-Santos, L.; Vizoso, A.F.; Camacho, E.M.; Piegari, L. Costs and feasibility of repowering wind farms. *Energy Sources Part B Econ. Plan. Policy* **2016**, *11*, 974–981. [[CrossRef](#)]
18. González-Longatt, F.; Wall, P.P.; Terzija, V. Wake effect in wind farm performance: Steady-state and dynamic behavior. *Renew. Energy* **2012**, *39*, 329–338. [[CrossRef](#)]
19. Lundquist, J.K.; DuVivier, K.K.; Kaffine, D.; Tomaszewski, J.M. Costs and consequences of wind turbine wake effects arising from uncoordinated wind energy development. *Nat. Energy* **2018**, *4*, 26–34. [[CrossRef](#)]
20. Vasel-Be-Hagh, A.; Archer, C.L. Wind farm hub height optimization. *Appl. Energy* **2017**, *195*, 905–921. [[CrossRef](#)]
21. Abbas, S.R.; Kazmi, S.A.A.; Naqvi, M.; Javed, A.; Naqvi, S.R.; Ullah, K.; Khan, T.U.R.; Shin, D.R. Impact Analysis of Large-Scale Wind Farms Integration in Weak Transmission Grid from Technical. *Energies* **2020**, *13*, 5513. [[CrossRef](#)]
22. Ouyang, J.; Li, M.; Zhang, Z.; Tang, T. Multi-timescale active and reactive power-coordinated control of large-scale wind integrated power system for severe wind speed fluctuation. *IEEE Access* **2019**, *7*, 51201–51210. [[CrossRef](#)]
23. Ameer, A.; Berrada, A.; Loudiyi, K.; Aggour, M. Analysis of renewable energy integration into the transmission network. *Electr. J.* **2019**, *32*, 106676. [[CrossRef](#)]
24. Chompoo-Inwai, C.; Yingvivanapong, C.; Methaprayoon, K.; Lee, W.J. Closure to discussion of Reactive compensation techniques to improve the ride-through capability of wind turbine during disturbance. *IEEE Trans. Ind. Appl.* **2005**, *41*, 1484. [[CrossRef](#)]
25. imen, L.; Djamel, L.; Zohra, M.; Selwa, F. Influence of the wind farm integration on load flow and voltage in electrical power system. *Int. J. Hydrogen Energy* **2016**, *41*, 12603–12617. [[CrossRef](#)]
26. Kraiczny, M.; Wang, H.; Schmidt, S.; Wirtz, F.; Braun, M. Reactive power management at the transmission-distribution interface with the support of distributed generators—A grid planning approach. *IET Gener. Transm. Distrib.* **2018**, *12*, 5949–5955. [[CrossRef](#)]
27. Prasai, A.; Sastry, J.; Divan, D.M. Dynamic capacitor (D-CAP): An integrated approach to reactive and harmonic compensation. *IEEE Trans. Ind. Appl.* **2010**, *46*, 2518–2525. [[CrossRef](#)]
28. Ouyang, J.; Tang, T.; Yao, J.; Li, M. Active Voltage Control for DFIG-based Wind Farm Integrated Power System by Coordinating Active and Reactive Powers under Wind Speed Variations. *IEEE Trans. Energy Convers.* **2019**, *34*, 1504–1511. [[CrossRef](#)]
29. She, X.; Huang, A.Q.; Wang, F.; Burgos, R. Wind energy system with integrated functions of active power transfer, reactive power compensation, and voltage conversion. *IEEE Trans. Ind. Electron.* **2013**, *60*, 4512–4524. [[CrossRef](#)]
30. Chen, B.; Fei, W.; Tian, C.; Yuan, J. Research on an Improved Hybrid Unified Power Flow Controller. *IEEE Trans. Ind. Appl.* **2018**, *54*, 5649–5660. [[CrossRef](#)]
31. Jowder, F.A.L. Influence of mode of operation of the SSSC on the small disturbance and transient stability of a radial power system. *IEEE Trans. Power Syst.* **2005**, *20*, 935–942. [[CrossRef](#)]
32. Mahela, O.P.; Shaik, A.G. Comprehensive overview of grid interfaced wind energy generation systems. *Renew. Sustain. Energy Rev.* **2016**, *57*, 260–281. [[CrossRef](#)]
33. Howard, D.F.; Jiaqi, L.; Harley, R.G. Short-circuit modeling of DFIGs with uninterrupted control. *IEEE J. Emerg. Sel. Top. Power Electron.* **2014**, *2*, 47–57. [[CrossRef](#)]
34. Liu, M.; Pan, W.; Quan, R.; Li, H.; Liu, T.; Yang, G. A Short-Circuit Calculation Method for DFIG-Based Wind Farms. *IEEE Access* **2018**, *6*, 52793–52800. [[CrossRef](#)]
35. Chrysochoidis-Antos, N.; Escudé, M.R.; van Wijk, A.J.M. Technical potential of on-site wind powered hydrogen producing refuelling stations in the Netherlands. *Int. J. Hydrogen Energy* **2020**, *45*, 25096–25108. [[CrossRef](#)]

36. Mendes, P.R.C.; Isorna, L.V.; Bordons, C.; Normey-Rico, J.E. Energy management of an experimental microgrid coupled to a V2G system. *J. Power Sources* **2016**, *327*, 702–713. [[CrossRef](#)]
37. Shehzad, M.F.; Abdelghany, M.B.; Liuzza, D.; Mariani, V.; Glielmo, L. Mixed Logic Dynamic Models for MPC Control of Wind Farm Hydrogen-Based Storage Systems. *Inventions* **2019**, *4*, 57. [[CrossRef](#)]
38. Quarton, C.J.; Tlili, O.; Welder, L.; Mansilla, C.; Blanco, H.; Heinrichs, H.; Leaver, J.; Samsatli, N.J.; Lucchese, P.; Robinius, M.; et al. The curious case of the conflicting roles of hydrogen in global energy scenarios. *Sustain. Energy Fuels* **2019**, *4*, 80–95. [[CrossRef](#)]
39. Apostolou, D.; Enevoldsen, P. The past, present and potential of hydrogen as a multifunctional storage application for wind power. *Renew. Sustain. Energy Rev.* **2019**, *112*, 917–929. [[CrossRef](#)]
40. Trifkovic, M.; Sheikhzadeh, M.; Nigim, K.; Daoutidis, P. Modeling and control of a renewable hybrid energy system with hydrogen storage. *IEEE Trans. Control Syst. Technol.* **2014**, *22*, 169–179. [[CrossRef](#)]
41. Castro-Santos, L.; Filgueira-Vizoso, A.; Carral-Couce, L.; Formoso, J.Á.F. Economic feasibility of floating offshore wind farms. *Energy* **2016**, *112*, 868–882. [[CrossRef](#)]
42. Myhr, A.; Bjerkseter, C.; Ågotnes, A.; Nygaard, T.A. Levelised cost of energy for offshore floating wind turbines in a life cycle perspective. *Renew. Energy* **2014**, *66*, 714–728. [[CrossRef](#)]
43. De Prada Gil, M.; Domínguez-García, J.L.; Díaz-González, F.; Aragués-Peñalba, M.; Gomis-Bellmunt, O. Feasibility analysis of offshore wind power plants with DC collectiongrid. *Renew. Energy* **2015**, *78*, 467–477. [[CrossRef](#)]
44. Kaldellis, J.K. *Stand-Alone and Hybrid Wind Energy Systems: Technology, Energy Storage and Applications*; Woodhead Publishing: Sawston, UK, 2010; Volume 554.
45. Ioannou, A.; Angus, A.; Brennan, F. Parametric CAPEX, OPEX, and LCOE expressions for offshore wind farms based on global deployment parameters. *Energy Sources Part B Econ. Plan. Policy* **2018**, *13*, 281–290. [[CrossRef](#)]
46. Projected Costs of Generating Electricity 2015—Analysis—IEA. Available online: <https://www.iea.org/reports/projected-costs-of-generating-electricity-2015> (accessed on 13 September 2021).
47. Böyük, G.; Mert, M. Fossil & renewable energy consumption, GHGs (greenhouse gases) and economic growth: Evidence from a panel of EU (European Union) countries. *Energy* **2014**, *74*, 439–446. [[CrossRef](#)]
48. Shayanmehr, S.; Henneberry, S.R.; Sabouni, M.S.; Foroushani, N.S. Drought, Climate Change, and Dryland Wheat Yield Response: An Econometric Approach. *Int. J. Environ. Res. Public Health* **2020**, *17*, 5264. [[CrossRef](#)]
49. Irtija, N.; Sangoleye, F.; Tsiropoulou, E.E. Contract-theoretic demand response management in smart grid systems. *IEEE Access* **2020**, *8*, 184976–184987. [[CrossRef](#)]
50. Wei, W.; Hao, S.; Yao, M.; Chen, W.; Wang, S.; Wang, Z.; Wang, Y.; Zhang, P. Unbalanced economic benefits and the electricity-related carbon emissions embodied in China’s interprovincial trade. *J. Environ. Manage.* **2020**, *263*, 110390. [[CrossRef](#)]
51. Georgatzis, V.V.; Stamboulis, Y.; Vetsikas, A. Examining the determinants of CO₂ emissions caused by the transport sector: Empirical evidence from 12 European countries. *Econ. Anal. Policy* **2020**, *65*, 11–20. [[CrossRef](#)]
52. Kumar, I.; Tyner, W.E.; Sinha, K.C. Input–output life cycle environmental assessment of greenhouse gas emissions from utility scale wind energy in the United States. *Energy Policy* **2016**, *89*, 294–301. [[CrossRef](#)]
53. Vargas, A.V.; Zenón, E.; Oswald, U.; Islas, J.M.; Güereca, L.P.; Manzini, F.L. Life cycle assessment: A case study of two wind turbines used in Mexico. *Appl. Therm. Eng.* **2015**, *75*, 1210–1216. [[CrossRef](#)]
54. Gomaa, M.R.; Rezk, H.; Mustafa, R.J.; Al-Dhaifallah, M. Evaluating the Environmental Impacts and Energy Performance of a Wind Farm System Utilizing the Life-Cycle Assessment Method: A Practical Case Study. *Energies* **2019**, *12*, 3263. [[CrossRef](#)]
55. Oebels, K.B.; Pacca, S. Life cycle assessment of an onshore wind farm located at the northeastern coast of Brazil. *Renew. Energy* **2013**, *53*, 60–70. [[CrossRef](#)]
56. Demir, N.; Taşkin, A. Life cycle assessment of wind turbines in Pınarbaşı-Kayseri. *J. Clean. Prod.* **2013**, *54*, 253–263. [[CrossRef](#)]
57. Hondo, H. Life cycle GHG emission analysis of power generation systems: Japanese case. *Energy* **2005**, *30*, 2042–2056. [[CrossRef](#)]
58. Al-Behadili, S.H.; El-Osta, W.B. Life Cycle Assessment of Dernah (Libya) wind farm. *Renew. Energy* **2015**, *83*, 1227–1233. [[CrossRef](#)]
59. Hadžić, N.; Kozmar, H.; Tomić, M. Offshore renewable energy in the Adriatic Sea with respect to the Croatian 2020 energy strategy. *Renew. Sustain. Energy Rev.* **2014**, *40*, 597–607. [[CrossRef](#)]
60. Mahfouz, M.M.; El-Sayed, M.A.H. Static synchronous compensator sizing for enhancement of fault ride-through capability and voltage stabilisation of fixed speed wind farms. *IET Renew. Power Gener.* **2014**, *8*, 1–9. [[CrossRef](#)]
61. 2010 to 2015 Government Policy: Low Carbon Technologies—GOV.UK. Available online: <https://www.gov.uk/government/publications/2010-to-2015-government-policy-low-carbon-technologies/2010-to-2015-government-policy-low-carbon-technologies#appendix-4-offshore-wind> (accessed on 20 September 2021).
62. NTDC, MERIT ORDER Based on Revised Fuel Prices, National Transmission and Dispatch Company Limited, Pakistan. 22 January, (2021). Available online: <https://ntdc.gov.pk/ntdc/public/uploads/services/meritorder/2021/January/MERIT%20ORDER%20WEF%2021%20JAN%202021.pdf> (accessed on 8 September 2021).
63. Ministry of Finance, Government of Pakistan. Economic Survey of Pakistan; 2021. Available online: https://www.finance.gov.pk/survey_2021.html (accessed on 8 September 2021).
64. Shaikh, F.; Ji, Q.; Fan, Y. The diagnosis of an electricity crisis and alternative energy development in Pakistan. *Renew. Sustain. Energy Rev.* **2015**, *52*, 1172–1185. [[CrossRef](#)]
65. Nosratabadi, S.M.; Hooshmand, R.A.; Gholipour, E. Stochastic profit-based scheduling of industrial virtual power plant using the best demand response strategy. *Appl. Energy* **2016**, *164*, 590–606. [[CrossRef](#)]

66. Huelo, Z.H.; Jiang, W.; Rehman, S. Technical and economic assessment of wind power potential of Nooriabad, Pakistan. *Energy. Sustain. Soc.* **2017**, *7*, 1–14. [[CrossRef](#)]
67. Internal Rate of Return (IRR) Definition & Formula. Available online: <https://www.investopedia.com/terms/i/irr.asp> (accessed on 4 October 2021).
68. Cai, L.J.; Erlich, I.; Stamtzis, G.C. Optimal choice and allocation of FACTS devices in deregulated electricity market using genetic algorithms. *2004 IEEE PES Power Syst. Conf. Expo.* **2004**, *1*, 201–207. [[CrossRef](#)]
69. Helmy, W.; Abbas, M.A.E. Optimal sizing of capacitor-bank types in the low voltage distribution networks using JAYA optimization. In Proceedings of the 2018 9th International Renewable Energy Congress (IREC), Hammamet, Tunisia, 20–22 March 2018; pp. 1–5. [[CrossRef](#)]
70. Ghiasi, M. Technical and economic evaluation of power quality performance using FACTS devices considering renewable micro-grids. *Renew. Energy Focus* **2019**, *29*, 49–62. [[CrossRef](#)]
71. Himri, Y.; Rehman, S.; Draoui, B.; Himri, S. Wind power potential assessment for three locations in Algeria. *Renew. Sustain. Energy Rev.* **2008**, *12*, 2495–2504. [[CrossRef](#)]
72. Clean Energy Project Analysis Third Edition RETScreen® Engineering & Cases Textbook. Available online: https://nrcaniets.blob.core.windows.net/iets/RETScreen_Engineering_e-textbook.pdf. (accessed on 17 September 2021).
73. Syed, A.H.; Javed, A.; Asim Feroz, R.M.; Calhoun, R. Partial repowering analysis of a wind farm by turbine hub height variation to mitigate neighboring wind farm wake interference using mesoscale simulations. *Appl. Energy* **2020**, *268*, 115050. [[CrossRef](#)]
74. Solid, M.; Power, W.; Sir, D.; Secretariat, P.; Division, C.; Secretariat, C.; Secretariat, P. National Electric Power Regulatory Authority Islamic Republic of Pakistan Determination of the Authority in the matter of Upfront Generation Tariff for. 2018, 5–7. Available online: <https://nepra.org.pk/tariff/Tariff/IPP/FFC%20Energy%20Ltd/TRF-156%20FFC%20EL%20COD%2010-11-2014%2014119-21.PDF>. (accessed on 17 September 2021).
75. Government of Pakistan Ministry of Planning, Development and Special Initiatives Pakistan Bureau of Statistics Press Release on Consumer Price Index (CPI) Inflation for the Month Analysis of Consumer Price Index (CPI) Base Year (2015-16) 2. 2020. Available online: <http://www.pbs.gov.pk> (accessed on 5 October 2021).
76. State Bank of Pakistan. Available online: <https://www.sbp.org.pk/sme/d/circulars/2016/C3.htm> (accessed on 5 October 2021).
77. National Electric Power Regulatory Authority Islamic Republic of Pakistan Registrar. Available online: www.nepa.org.pk (accessed on 5 October 2021).
78. Rules, P.; Electric, N.; Act, E.P. National Electric Power Regulatory Authority Schedule. *Cell* **2002**, *385*, 3–6. Available online: [https://nepra.org.pk/Legislation/2-Rules/2.4%20NEPRA%20\(Fees\)%20Rules,%202002/NEPRA%20Fee%20Rules%20along%20with%20amendment%202020.pdf](https://nepra.org.pk/Legislation/2-Rules/2.4%20NEPRA%20(Fees)%20Rules,%202002/NEPRA%20Fee%20Rules%20along%20with%20amendment%202020.pdf) (accessed on 17 September 2021).
79. NEPRA Grid Code Addendum No. 1 for Grid Integration of Wind Power Plants, April 2010. Available online: <https://nepra.org.pk/Standards/Codes/NTDC-GRID%20CODE%20ADDENDUM%20NO%201.PDF> (accessed on 5 October 2021).
80. Saqib, M.A.; Saleem, A.Z. Power-quality issues and the need for reactive-power compensation in the grid integration of wind power. *Renew. Sustain. Energy Rev.* **2015**, *43*, 51–64. [[CrossRef](#)]